THE INFLUENCE OF RESTRICTIONS ON THE BREAKUP PATTERN OF TURBULENT WATER JETS

A SIMPLE MODEL OF THE EXTERNAL URINARY STREAM OF THE HUMAN MALE

Verslag van het afstudeerwerk voor het ingenieursexamen van de werktuigbouwkundige afdeling van de Technische Hogeschool te Delft, verricht onder leiding van Prof. Ir. J. O. Hinze en Ir. H. Leijdens.

H. Vliem,
Leiden, mei 1975.

CONTENTS

I.	Introduction
I. A.	Purpose of this investigation
I. B.	Earlier work
II.	Experimental
II. A.	Apparatus
II. A. 1	Flowsystem
II. A. 2	Restrictions and modifications of the test section
II. A. 3	Laboratory Drop Spectrometer
II. A. 4	High speed photography
II. B.	Summary of experiments
II. C.	General procedure
III.	Analysis
III. A.	Preliminary digital analysis
III. A. 1	A/D conversion
III. A. 2	Analysis
III. B.	Statistical treatment of the output
III. B. 1	Standard mean difference
III. B. 2	Discriminant procedures
IV.	Experiments and results
IV. A.	Sensitivity of measurements to experimental conditions
IV. A. 1	Measurements
IV. A. 2	Results
IV. B.	The effect of restriction 5 when placed 10, 20, 30, 40, and 50 diameters upstream from the tube orifice
IV. B. 1	Measurements
IV. B. 2	Results
IV. C.	The effect of the different rigid restrictions when placed 10 and 40 diameters upstream from the tube orifice
IV. C. 1	Measurements

IV. C. 2 Results
IV. D. The effect of self-exciting oscillations of the elastic restriction
IV. D. 1 Measurements
IV. D. 2 Results
IV. E. The effect of the fossa navicularis and elliptical meatus
IV. E. 1 Measurements
IV. E. 2 Results
IV. F. Breakup lengths

V. Succeeding investigations

VI. Conclusions
VI. A. Specific conclusions
VI. A. 1 The effect of restriction 5 when placed 10, 20, 30, 40, and 50 diameters upstream from the tube orifice
VI. A. 2 The effect of the different restrictions when placed 10 and 40 diameters upstream from the tube orifice
VI. A. 3 The effect of self-exciting oscillations of the elastic restriction
VI. A. 4 The effect of the fossa navicularis and elliptical meatus
VI. A. 5 Analysis of the recorded data
VI. B. Comparison between the experiments with air and water
VI. C. Final conclusions

Appendix 1
Basic principles of the optical-electro transducer

Appendix 2
Estimation of the initial disturbance amplitude

I. Introduction

Urethral strictures are a common source of lower urinary tract disfunction (Campbell, 1970). Such strictures can occur as congenital defects or result from infection, inflammation, or glandular hypertrophy. Conventional methods for the diagnosis of urethral strictures are time consuming, uncomfortable for the patient and, as they are invasive techniques, carry certain risks.

In the last three years the Academic Hospital in Leiden has been evaluating a noninvasive method, called "Urinary Drop Spectrometry" (U.D.S.), as an alternative to the conventional techniques for initial screening and diagnosis of lower urinary tract obstruction. The method of drop spectrometry is based on the observation of the external urinary stream by means of an electro-optical instrument. Since the external stream breaks up into drops shortly after leaving the urethral meatus, the resulting sequence of drops can be transduced to a sequence of electrical pulses, in which the statistical properties of drop frequency, size, spacing, oscillation, etc. are imbedded. By empirical correlation between the statistical properties of the drop sequence and conventional diagnostic techniques, the method has been developed to the stage where gross diagnosis is possible and the effect of patient treatment can be traced. For further improvement in the diagnostic capability, however, a more fundamental understanding of the physiological and hydrodynamic processes is necessary.

I. A. Purpose of this investigation

It has been assumed that the variation in the observed U.D.S. patterns is due, in part, to an alteration of the turbulent structure in the flow downstream from a stricture and thus to an alteration of the turbulence in the emerging jet. This alteration in turbulence may, in turn, influence the breakup pattern. To test the plausibility of this assumption, an investigation has been carried out in two stages:

1. R.C.D. Lissenburg has studied the influence of an obstruction on the structure of turbulent pipe flow in air. The size and shape of the obstruction, the distance downstream from the obstruction and the physical characteristics of the canal were variables which were investigated. His results will be discussed in section B of this chapter.

2. In this investigation, we have scaled the experiments of Lissenburg, geometrically and dynamically, to turbulent pipe flow of water and have studied the effect of the known alterations in the turbulent structure on the process of jet breakup. In the present experiments the characteristic dimensions closely approximate the characteristic dimensions of the human male urethra; this assures that dynamic similarity to human urination is also maintained. The effects of the turbulence have been studied by measuring and analyzing the patterns in the drops of the disrupted jet.

I. B. Earlier work

Despite the many theoretical and experimental investigations on the capillary instability of liquid jets, there is not yet a comprehensive theory for the phenomenon. Experimental measurements are most commonly presented in the form of a breakup curve (fig. I. 1) which relates the length of the continuous portion of the jet to its velocity. The breakup curve can be conveniently divided into three regions; a laminar region, a transition region and a turbulent region.

The laminar breakup has been the most intensively studied. At low velocities, the jet length is linearly related to the jet velocity (laminar region). At higher velocities, the length - velocity relation departs from a linear behaviour and, at some critical velocity, reaches a maximum (transition region).

Rayleigh (1878) laid the analytical foundations for the capillary instability of liquid jets through a perturbation analysis of the inviscid form of the equations of motion. He showed that only axisymmetric disturbances are unstable, and that any axisymmetric disturbance whose wavelength was greater than the circumference of the jet would grow and eventually lead to breakup.
The growth rate of the disturbance, and thus the breakup time, was found to depend only on the jet dimension and fluid properties and was independent of the velocity. As the jet length is equal to the product of the breakup time and the velocity, a linear length - velocity relation is predicted. A critical feature of Rayleighs analysis is the dependence of the growth rate on the wavelength of a disturbance. A disturbance whose wavelength is equal to 4.51 times the jet diameter was found to grow fastest and, providing all disturbances have the same initial amplitude (white noise), this most unstable disturbance will dominate the jet breakup. The jet should then break into drops separated by the distance

$$\lambda^* = 4.51\ D_j.$$

Continuity of mass demands that the drops have the volume and diameter

$$V_d = \frac{\pi}{4} D_j^2 \lambda^* = 3.54\ D_j^3 \qquad D_d = 1.89\ D_j.$$

The drop frequency can be expressed in terms of the Strouhal number;

$$Sr = \frac{f\ D_j}{\bar{U}_j}$$

Since the drop frequency is equal to $\bar{U}_j/\lambda^*$, we have for the Rayleigh breakup

$$Sr^* = D_j/\lambda^* = (4.51)^{-1}.$$

Furthermore, the jet will be unstable to all disturbances with $\lambda > \pi D_j$; i.e. for $Sr_{crt} < \pi^{-1}$.

Weber (1931) attacked two of the defiencies in Rayleighs analysis. He first extended the analysis to include the effect of viscosity, an effect treated by Rayleigh only in the limit as the viscosity tends toward infinity. Webers result agrees well with experimental measurements in the linear part of the breakup curve and shows that for water jets the viscous correction can be ignored. In the second part of his analysis, Weber considered the aerodynamic forces on the jet, i.e. the effect of the relative motion between the jet and the air. He found that the aerodynamic forces enhance the growth rate of axisymmetric disturbances and his theory indeed predicts a maximum in the breakup curve. The theoretical and experimental values of the maximum length and the velocity for which the length is maximum, however, failed to agree. Sterling (1975) has modified Webers analysis to account for the viscosity of the ambient fluid; the results of his modified analysis agree well with experimental values. It was found that aerodynamic forces could be ignored provided the Weber number based on the ambient density, $\hat{We} = \frac{\rho_a D_j U_j^2}{\sigma}$, was less than 1.

Dityakin (1954) has investigated, theoretically, the effect of nozzle ellipticity and has shown that if the excentricity ($c = \sqrt{1-b^2/a^2}$, a and b are the major and minor axis) is increased, the jet length will be shorter and the most unstable wavelength smaller. Thus the drops will be smaller and the drop frequency higher.

Lafrance (1974) has obtained a solution of the equations of motion to third order in the perturbations. He has found that the effective growth rate of disturbances is very close to that predicted by the linear theory and that the drop sizes can be predicted well as a function of the wavelength of an initial disturbance.

When the jet becomes turbulent, the breakup length is first sharply reduced and then increased linearly with velocity. The sudden decrease in the jet length is commonly attributed to the large amplitude disturbance of the jet surface by turbulent eddies. The study of turbulent jets has been mostly limited to high speed jets (in application to atomization of fuels). There are a few studies on the behaviour at low or intermediate Reynolds number and these are largely limited to the length - velocity relationships.

Chen (1964) has found for a turbulent jet, that "the increasing size of the surface disturbance as the jet travels downstream is due to the propagation of the large scale turbulence distributed within the jet. After the influence of the largest scale turbulence is felt, the surface disturbance due to the internal turbulence ceases to grow, and varicose breakup mechanism continues to desintegrate the jet, producing the initial drop. From the orifice to the breakup point, the initial disturbance of the jet due to turbulence in the fluid and the surface tension forces are thus the predominant factors...".

Van de Zande (1974) has studied the effect of nozzle length on the breakup length of low Reynolds number turbulent jets. With increasing nozzle length he has found the transition from laminar to turbulent flow is shifting to the region of lower jet velocities. The more fully developed the turbulence at the orifice, the stronger will be the initial disturbance of the jet and thus the shorter will be the breakup length.

It is clear that, to understand better the effect of turbulence on the breakup process, it is important that the turbulent structure within the issuing jet is known. This information is provided by the study of Lissenburg, i.e. stage 1.

Lissenburg (1974) has studied the influence of a restriction on the structure of turbulent pipe flow of air. He has found that, in the turbulent structure of the flow in a tube, the influence of a rigid

restriction can be observed at the centreline as far as 40 tube diameters downstream of the restriction and near the wall about 20 tube diameters downstream. The shape of the restriction influenced the turbulence such that the more gradually the restriction decreased in the downstream direction, the more persistent were the effects.

The observed effects are most pronounced in the low frequency range ($Sr < 1$). In this range, the turbulent structure does not monotonically approach the fully developed structure with increasing distance downstream from a restriction. Rather, there is first a decrease in the turbulent energy until about 10 diameters, then an increase in energy to a maximum at about 25 diameters, then again a monotonic decrease to the fully developed value.

Wall roughness obscures the effect of a restriction such that increasing the wall roughness of the tube is similar to increasing the distance between the restriction and the end cross section.

If the circular cross section of the tube is brought smoothly to an elliptical cross section (designed to simulate the geometric configuration at the downstream end of the urethra, i.e. the fossa navicularis and meatus) there is a damping of the turbulent energy in the entire wavenumber range. Again the effects are most pronounced in the low frequency range.

He has found further that periodic oscillations induced by vibrating systems are very persistent and are observed for more than 50 tube diameters downstream, even near the wall. Wall roughness, tube curvature and the fossa navicularis had little effect on these periodic phenomena.

II. Experimental

The aim of this investigation was to find a possible correlation between known alterations in the turbulent structure of a low Reynolds number pipeflow and the breakup pattern of the jet. Thus the same test conditions have been used here as were used by Lissenburg; i.e. the Reynolds number Re_D for the turbulent pipeflow was set to a constant value of 5000 and the restrictions used by Lissenburg have been scaled geometrically. All experimental variables, except for the modification of the test section with the restrictions, were held constant throughout the investigation. Thus any alteration of the jet breakup must be due to the effect of the restrictions.
The series of experiments carried out can be divided roughly into three parts:

1. The effect on the jet breakup for a given restriction as a function of the location of this restriction in the tube,
2. The effect on the jet breakup of the shape of a restriction, placed at a given distance from the orifice of the tube,
3. The effect on the jet breakup for a periodic disturbance caused by an oscillating restriction.

A flowchart of the experimental procedures is given in fig. II.1.

For the examination of the jet breakup we have used a small "Laboratory Drop Spectrometer" (L.D.S.). For a better understanding of the phenomena occurring in the jet, high speed ciné and a stroboscope were also used (section I of fig. II. 1).
The electrical signal of the L.D.S. has been analyzed either by special analog instruments routinely used for patient examination or by a detailed analysis on a IBM 370/154 computor (section II).
The output of the digital computor analysis has been screened and the results analyzed statistically (section III).

II. A. Apparatus

II. A. 1. Flowsystem

The flowsystem consists of a water supply, a flowmeter, a calming chamber and a test section, a schematic diagram is given in fig. II. 2.

Water supply

The liquid source was an open tank (A) placed three meters above the floor. The input of the tank was from the normal water supply. In the tank a constant level was maintained by an overflow system (B), two meters above the exit of the test section. Because the two meter pressurehead was insufficient, in some extreme cases, a direct connection (C) between the output of the tank and the normal water supply was provided.

The flow to the test section was controlled by a valve (D) and measured by a variable area, glass tube flowmeter (E). The flowmeter was linear over the working range of flow values (fig. II. 3). When use was made of the normal water supply by connection (C), it was noticed by observing the flowmeter that the fluctuation of the flowrate was about the same as when the constant headtank was used, (fluctuations were less than 0.5% full scale).

The connection between the calming chamber (F) and the valve (D) was made of a flexible tube; this allowed the apparatus to be handled more easily. The calming chamber was designed to provide a uniform, laminar flow to the entrance tube of the test section. Therefore the diameter of the calming chamber was chosen about 15 times the diameter of the entrance tube of the test section. Moreover, the upper half of the calming chamber was filled with crumpled plastic netting (usually sold as pancleaners), while the under half was empty. The two parts are divided by a plastic screen of meshsize 1.5 mm (D = 0.25 mm).

Test section

The test section (G) was coupled directly to the calming chamber by an entrance tube (I.D. = 5 mm). The test section was held in a vertical position with the jet directed downward.
When ink was injected into the flexible tube, near the entrance of the calming chamber, the water in the under half of the calming chamber coloured uniformly. Thus the velocity profile formation in the entrance tube of the test section wasn't disturbed by direct streamlines from flexible tube to entrance tube.
Initial observations of the jet formed by this flowsystem showed that the turbulence was sometimes intermittent. In order to ensure turbulence in the test section a screen of 1.5 mm meshsize (D = 0.25 mm) was placed at the beginning of the entrance tube of the test section, while the first 25 mm of the entrance tube were roughened by machining V shaped grooves in the wall.
Precautions were not taken to ensure for fully developed turbulent pipeflow at the most upstream location of the restrictions. Indeed, this location is only 23 tube diameters downstream from the calming chamber and 10 tube diameters downstream from the 1 mm diameter reduction from the entrance tube to the test section. However, as the flowrate was held constant for every measurement, for a given location the turbulent velocity profile also was constant and the effect of a restriction on this given profile could be measured.

The test section, calming chamber and most of the water supply were made of transparant polyvinylchloride.

Calibrating the test section

In order to maintain dynamic similarity between the present experiments and the experiments of Lissenburg, the Reynolds number (based on the tube diameter) was held constant at $Re_D = 5000$. Since

$$Re_D = \frac{\bar{U}_T \, D}{\nu}$$

and

$$\bar{U}_T = \bar{Q}/(\pi D^2/4)$$

we have

$$\bar{Q} = \frac{\pi D \nu}{4} \mathrm{Re}$$

Furthermore, in order to maintain dynamic similarity between the present experiments and the external urinary stream, we take D = 4 mm. For water we have $\nu = 1.10^{-6}$ thus

$$\bar{U}_T = 1.26 \text{ m/s}$$

and $$\bar{Q} = 15.7 \text{ ml/s}.$$

This values are within the range of a "normal" urination. The Weber number based on the ambient density, ρ_a, becomes

$$\hat{We} = \frac{\rho_a D_j U_j^2}{\sigma} \simeq 0.1$$

Thus aerodynamic forces are unimportant.

It is clear that gravitational forces will affect the breakup process through a thinning of the jet as it accelerates; the longer the continuous portion of the jet, the more pronounced will be this effect. In the present experiments, however, the continuous jet length was nearly the same for all measurements and, as we are looking only for differences in the jet breakup with modification of the test section, acceleration effects can be ignored.

II. A. 2. Restrictions and modifications of the test section

Since the test section was intended to simulate in a very rough

way the human male urethra, the L/D ratio of the tube (D = 4 mm) was set at 60. The straight open tube simulated the normal male urethra and therefore it was the standard configuration to which other configurations were compared. Strictures in the urethra were simulated by placing restrictions of different size, shape and rigidity at various locations in the test section.
Since Lissenburg has found that a possible effect of a rigid restriction is obscured by wall roughness and that this wall roughness has little effect on periodic phenomena, no wall roughness has been introduced in the test section.

Rigid restrictions

In figure II. 4 the five types of rigid restrictions which were investigated are shown.
Restriction 1 simulates a membranous stricture or valve and restriction 2 a fibrous stricture as does restriction 5. In order to investigate whether the effect of restriction 5 was due to the converging and diverging part, restriction 3 and 4 were also used. All these restrictions were made of a Cu-Al alloyage.

Elastic restriction and fossa navicularis with elliptical meatus (fig. II. 5)

An elastic restriction was constructed to test the effect of the spontaneous vibrations found by Lissenburg. The shape is almost the same as restriction 5. This restriction was constructed by placing a specially made rubber tube of 0.05 mm wall thickness and with an inside diameter of 4 mm, inside a piece of 5 D length and 4.1 mm diameter transparant P.V.C. tube. The connections of the rubber on the plastic tube were constructed by turning up the rubber tube ends and glueing these to the plastic tube.
A fossa navicularis with an elliptical meatus, geometrically similar to the one used by Lissenburg, is also tested. This is placed at the end of the tube. In the Y-Y plane there is first a widening and then a

slight contraction. In the Z-Z plane there is only a smooth contraction. Together with the elliptical form of the meatus, the fossa navicularis can act as a calming chamber and therefore change the flow pattern substantially.
A 5 mm diameter stainless steel tube was used for the test section to provide a smooth connection between tube and fossa navicularis.

II. A. 3. Laboratory Drop Spectrometer

A schematic review of the L.D.S. transducer and amplifier is given in fig. II. 6 and 7. The principle of the L.D.S. is based on the interception by a droplet of a light sheet which is directed on the sensitive part of a photodiode.
The almost spherical beam of a small lightsource (A) is converted to a nearly homogeneous lightfield by a system of a doublet lens (B) and a thin slit (C). A second slit (D) is placed just before the photodiode (E) to reduce light reflections from the drops and most of the non-parallelism of the lightfield. As the slits have a width of 0.2 mm the thickness of the beam is small compared with the diameter of a typical drop. Thus the amount of light intercepted by the drop (and thus the amplitude of the signal from the photodiode) is proportional to the local width of a drop in a plane of the light sheet and parallel to the detector (see appendix 1).

To reduce the pickup of radiated electromagnetic energy, the first stage (F) of a four stage amplifier is placed inside the L.D.S. and enclosed by a grounded metal box. Also two stages of active filtering at 10 khz reduce both the noise level of sharp spikes from power line hash and radiant pickup.
The negative pulses are about a tenth of a volt superposed on the 7 to 8 Volt D.C. level of the activated photodiode. The D.C. level is removed, the pulses inverted and amplified and the signal is clamped to a zero level baseline. A final amplifier provides the adjustment of the output voltage. System noise is about 0.5% the height of the standard calibration

pulse (see below), which results in a S/N ratio of about 50 dB, in practice the noise performance has been limited by the S/N ratio of the FM recorder (45 dB).

Calibrating the L.D.S.

In calibrating the L.D.S., two aspects must be considered;

1. The homogeneity and parallelism of the light sheet,
2. The output of the amplifier related to a constant interruption of the light sheet.

re 1) The slit (E) and the photodiode were adjusted against each other until the light sheet received by the photodiode was homogeneous within 2% over a width of 50 mm. This has been measured by dropping from a constant height a $\frac{1}{4}$ inch ball, at several transverse positions within the lightfield. The resulting pulses were stored on an oscilloscope and compared. If the deviation of the pulse height was greater than 2%, the optical components were readjusted.

re 2) The gain of the amplifier was adjusted so that the output pulse from this $\frac{1}{4}$ inch ball was 0.50 Volt. The pulse height was measured from a stored trace on a calibrated oscilloscope.

II. A. 4. High speed photography

For a better understanding of the physical phenomena occurring as a liquid jet leaves an orifice, two kinds of photography has been used; high speed ciné with a Hitachi camera and high speed photography with a Strobodrum camera.

II. B. Summary of experiments

1. Sensitivity of measurements to experimental conditions.

A liquid jet and especially a turbulent jet doesn't show break-up at a unique downstream point. Rather, there is a variation in the breakup length. Beyond the initial breakup point, some drops and threads of liquid show a secondary drop breakup and the drop pattern changes. Thus the minimum distance from the tube orifice for the drop pattern to become stable should be known. Once a certain distance for recording the drop pattern is chosen, this distance must be kept constant for the whole series of experiments.
To determine this distance, the following experiments have been carried out.

a. The L.D.S. has been located at several distances from the tube orifice and recordings of the drop pattern have been made.

b. A high speed ciné has been made of the discontinuous part of the jet.

Furthermore the measurements should be reproduceable. Therefore some preliminary analyses of drop patterns, recorded several weeks apart, have been carried out.

2. The effect of restriction 5 when placed 10, 20, 30, 40 and 50 diameters upstream from the tube orifice.

3. The effect of the different rigid restrictions when placed 10 and 40 diameters upstream from the tube orifice.

4. The effect of a self-exciting oscillation of the elastic restriction.

5. The effect of the fossa navicularis and elliptical meatus.

6. Breakup lengths.

II. C. General procedure.

In general, the procedure of the measurements was as follows:

1) Calibrate L.D.S. system and record four or five calibration pulses (0.50 Volt) of the $\frac{1}{4}$ inch ball.
2) Establish a given configuration of the test section.
3) Position L.D.S.
4) Adjust liquid flow to get the right Reynolds number.
5) Record data for 1 minute.
6) Change configuration of the test section and repeat steps 2 to 6.
7) Data analysis.

re 5) The signal of the L.D.S. system has been recorded on a Hewlett Packard 3960 FM Tape Recorder at a recording speed of 15 inches per second. Voice annotation was used to label the data.

re 6) To reduce symptomatic errors in the measurements, each experiment was divided into at least 4 parts. For example, when the location of the restriction was varied, the sequence of measurements was as follows.
One minute of data segments were recorded, first with no restriction in the tube, then with the restriction placed 10 diameters from the orifice, then 20 diameters from the orifice, etc., and finally with the restriction 50 diameters from the orifice. The obstruction was then removed and the entire sequence repeated, at least 4 times.

III. Analysis

The recorded data, for the most part, have been analyzed digitally on an IBM 370 computor. However, sometimes use has been made of special analog instruments that are also used for patient examination. These instruments analyze only the pulses above a certain constant trigger level; the small drops are neglected. The output consist of:

1) the number of big drops.
2) the frequency of the drops passing by the lightfield of the L.D.S.
3) a histogram of the time intervals between the big drops.

III. A. Preliminary digital analysis

III. A. 1. A.D. conversion

The signal of the magnetic tape has been converted from analog to digital by an IBM 1800 computor. The digitizing rate was set to be 5,000 Hz and the voltage resolution was about 22,500 units per Volt. Before digitizing, the output gain of the FM recorder was checked to ensure that the calibration pulses had an amplitude of 0.50 Volts. The one minute analog data set for each configuration has been reduced to 180 blocks of digital data. Each block consisted of 1024 words and at the converting factor of 5,000 Hz, its duration was $\frac{1024}{5000}$ sec. Each set of 180 blocks was preceded by a label block to identify the experimental run. The digitized data have been written on digital magnetic tape.

III. A. 2. Analysis

The digitized data have been analyzed on an IBM 370 computor. The software for these analysis was developed by Prof. J. van Ness as part of an earlier investigation of data from the urology department.

A flow chart for the program is given in fig. III. 1, while in fig. III. 2 an outline is given for the treatment of the pulse train from L.D.S. to final output.
In the program, the pulse train is examined and for each pulse above a certain trigger level (0.005 Volts), the pulse height, the centroid of the pulse, the time since the preceding pulse and the time at which the pulse begins and ends has been computed. One data set of 180 blocks was divided in 12 groups of 15 blocks, over which groups the means and standard deviations for each variable has been computed. Furthermore the mean value and standard deviation of the signal has been calculated, and the spectra of the beginning and end vector of the group has been computed. All these data of one group have been written on magnetic tape. For each experiment the mean values and standard deviations of the number of drops, the pulse height, the spacing, the signal, the spectrum and the histograms of the time interval and pulse height distribution have also been punched on cards and listed on hard-copy output.

III. B. Statistical treatment of the output

Because the number of variables was too large to survey what the difference was between two or more configurations, a statistical analysis has been carried out consisting of three parts. This should select the variables which differentiate best between the configurations which were used.

III. B. 1. Standard mean difference

Between each pair of configurations the standard mean difference for each of the variables has been calculated.
For n measurements of variable X we have.

Mean of X: $\bar{X} = \frac{1}{n} \sum_{k=1}^{n} X_k$

$$\text{standard deviation } S = \sqrt{\frac{1}{n-1} \sum_{k=1}^{n} (X_k - \bar{X})^2}$$

The Standard Mean Difference for X between two configurations i and j is defined as

$$S.M.D. = \frac{|\bar{X}_i - \bar{X}_j|}{\sqrt{S_i \cdot S_j}}$$

A careful interpretation of all the S.M.D.'s should tell us if there is a significant difference in the breakup process for the different configuration. A better interpretation can be obtained by taking for example the 35 variables with the largest SMD and fed these to some statistical discriminant procedures as shown below.

III. B. 2. Discriminant procedures

We have used the 35 selected variables and have entered these variables for each group of each configuration into a stepwise, discriminant analysis. This analysis selects, in their order of discrimination power, the variables which best distinguish between the configurations under consideration. By dividing the total number of groups for each configuration into two parts, one for training data, the other part for test data, the classification of these test data was our final result. If the classification of these test data into the true configuration could be done better by this procedure than by pure chance, this was an indication of a difference in breakup pattern.

For this final analysis we have used two kinds of discriminant procedures, a linear and a non-linear. The difference between these two methods is the form at the boundary planes between the variables of each configuration. For example if there are two configurations the mean values for one variable can be calculated for each group. The linear procedure has a hyperplane between the two configurations while for the non-linear method the curvature of a hypersurfaces can be chosen.

For the linear discriminant analysis we have used a program: BMD07M Stepwise Discriminant Analysis, Health Sciences Computing Facility, UCLA. For the non-linear method use has been made of a program written by the statists of the Centraal Reken Instituut Leiden. The linear discriminant analysis was used to eliminate 25 of the initial 35 variables and with the remained 10 variables we have used the non-linear discriminant analysis. For this final analysis all the groups of one configuration are training data except one group which have to be classified. Doing this several times, each with another group as test data, this analysis gives the most important variables and the most probable classification of each group for these variables.

IV. Experiments and results

In this chapter the specific procedures and specific results will be described for each of the experiments. For all the experiments the water temperature was held at $15^{o}C \pm 1^{o}C$. In this temperature range the physical properties of water could be regarded as constant. Since the water was drawn from the normal water supply the chemical properties could also be regarded as constant. The Reynolds number for the turbulent pipeflow was set at 5,000 (except for a few special experiments discussed later). Any change in the breakup pattern from one experiment to another was attributed only to the change in the turbulent structure of the pipeflow.

Survey of experiments

1) Sensitivity of measurements to experimental conditions.
2) The effect of restriction 5 when placed 10, 20, 30, 40 and 50 diameters upstream from the tube orifice.
3) The effect of the different rigid restrictions when placed 10 and 40 diameters upstream from the tube orifice.
4) The effect of a self-exciting oscillation of the elastic restriction.
5) The effect of the fossa navicularis with elliptical meatus.
6) Breakup lengths.

IV. A. Sensitivity of measurements to experimental conditions

In order to know the location where the drop pattern becomes stable, the following experiments were carried out.

IV. A. 1. Measurements

The distance between the L.D.S. and the tube exit was varied from

0.2 m (the breakup point) to 0.42 m in four steps of 0.08 m. At each location the drop pattern was recorded for both the open tube at a Re_D = 7400 and with restriction 1 placed at the orifice of the tube at a Re_D = 4200. The data were analyzed by the analog hospital instruments.
In addition to these experiments a high speed ciné was made of the discontinuous part of the jet from the open tube at Re_D = 7400.

IV. A. 2. Results

The data acquired by the L.D.S. and analyzed by the analog hospital instruments are shown in fig. IV. 1 and 2. The results of the high speed ciné are shown in fig. IV. 3. By tracing the path of each drop, a history of drops formed at certain place and time has been made. This history clearly showed the secondary drop breakup and it sometimes appeared that secondary breakup followed drop coalescence. However, it was not clear whether this was indeed a coalescence or simply an elastic collision between two drops. The history also shows a tendency for the drops to travel in clusters. The reason for it could be natural or some unobserved pressure fluctuations in the water supply. In the further experiments, no such phenomenon was observed either by visual inspection of the jet with a stroboscope or by analysis of the spectral distribution and the spectrum of the pulse beginnings and ends. From the history it can be concluded that from a distance of about 0.30 m from the tube orifice the breakup pattern is sufficient stable. In the spectral distributions, however, the difference in the drop pattern becomes small only for distances greater than 0.6 m from the tube orifice; at this distance the breakup pattern is stable. The difference between fig. IV. 1 and fig. IV. 2 could be expected because restriction 1 placed at the tube orifice, acts as an orifice with diameter half that of the open tube and therefore produces smaller drops and a faster stream than the open tube does.
It was determined, mostly from the high speed ciné, that a distance of about 0.45 m from the tube orifice would be sufficient to provide an

almost stable drop pattern.
The reproduceability of the measurements has also been tested. In some preliminary experiments a few recordings of the drop pattern from the tube without restriction were made, several weeks apart. There were small but monotonic changes in the patterns with time. To avoid the complications which such "aging" effects would introduce into the analysis, all experiments for which drop patterns were compared were completed within two hours.

IV. B. The effect of restriction 5 when placed 10, 20, 30, 40 and 50 diameters upstream from the tube orifice

For this experiment we have chosen restriction 5 because Lissenburg has found for this restriction still a change in the turbulent structure at the orifice when the restriction was located at a distance of 40 diameters upstream from the orifice.

IV. B. 1. Measurements

Of each configuration i.e. the restriction located at a given distance from the tube orifice, six recordings of the drop pattern have been made. The sequence was as follows: open tube, L/D = 10, 20, etc., 50; open tube, L/D = 10, etc.

IV. B. 2. Results

The data obtained for the drop pattern with restriction 5 placed at 10, 20, 30, 40, and 50 diameters upstream from the orifice are given in figures IV. 4 and 5 and tables IV. 1 and 2 together with the data obtained for the open tube.

Clearly, a variation in the location of the restriction does not lead to large differences in the drop pattern. Thus the much

greater differences in the pattern observed with patients cannot be attributed simply to a variation in the location of an obstruction.

The pulse height distribution (fig. IV. 4) has a typical bimodal form, i.e. the discontinuous stream consists of large "main" drops and small "satellite" drops. Whereas they are observable differences in the distributions, there are no monotonic or systematic changes with the location of the restriction. The data are, however, nearly bounded by the distributions for L/D = 10 and L/D = 30; the drops for L/D = 30 are smaller and the mode for the satellite drops is narrower. This agrees qualitatively with the results of Lissenburg that the ratio of low frequency to high frequency turbulent energy is a minimum for L/D = 10 and maximum near L/D = 30.

The shape of the time interval distribution (fig. IV. 5) suggests that the drop arrival times are Poisson distributed. The time interval distributions for all configurations are nearly identical.

The plots of the spectra of the pulse beginnings and ends vector aren't given because the differences for the curves of different configurations are small and no visual information can be drawn. The same holds true for the time interval distributions.

The change in every variable with a change in the location of the restriction is small (table IV. 1); there is no single variable, which clearly distinguishes the location of the restriction. That is, the standard mean differences for all variables and for all configurations are small. Thus it is necessary to apply a multivariable analysis to see if systematic differences exist. The results for both the linear and non-linear discriminant analyses are given in table IV. 2.

Linear discriminant method

Three matrices are given A, B, and C. For A and B the same variables were used. Matrix A is the classification after the selection of the 10 variables which best distinguish, while for matrix B all the 35 variables were used. The difference between the two matrices can be explained by the number of variables, 35 variables are too many for only 48 groups.
Within the 10 best variables there are 5 from the pulse height distribution, so an analysis is carried out with variables chosen only from the pulse height distribution; matrix C. These three matrices show, in the diagonal, a sudden decrease in correct classification when the restriction was placed more than 20 diameters upstream. At this and greater distances the different patterns are difficult to separate. That is, it is difficult to determine if the restriction is at L/D = 30, 40, or 50 but it is more clear that the restriction is not at L/D = 10 or 20.

Non-linear discriminant method (matrix D)

When the 10 best variables of the linear discriminant analysis were entered in a non-linear discriminant method, two variables from the spectra of the pulse beginnings and ends vector are first chosen followed by a variable from the pulse height distribution. A result, not fully explained, is the much better classification of the patterns for the location 20 and 50 diameters upstream from the orifice. The matrix A shows the same but smaller effect. The matrix D shows that only the pattern for the location L/D = 20 is unique, while the patterns for the other locations look, for the most part, like the patterns for the location L/D = 50.

IV. C. The effect of the different rigid restrictions when placed 10 and 40 diameters upstream from the tube orifice

The aim of this investigation has been twofold:

1) the effect of different shape and size of a restriction on the breakup pattern.

2) comparison between the restrictions for the persistancy of a possible change in breakup pattern, when the distance between the location of the restriction and the tube orifice has been increased.

IV. C. 1. Measurements

At both locations four recordings of the breakup pattern have been made for each restriction. The recording sequence was as follows: open tube, restriction 1 placed 10 diameters upstream from the tube orifice, restriction 1 placed at 40 diameters upstream, restriction 1 placed 10 diameters upstream, etc. (four times), then open tube again followed by restriction 2 placed 10 diameters upstream, etc., until restriction 5.
For restriction 1 the two-meter pressure head was to low to provide a Reynolds number of 5000. Only for this restriction the recordings of the breakup pattern have been made while the desired flow rate was supplied by the normal water supply.
The variables that were used in the statistical analysis were for both locations the same. They have been gathered from the analysis of the data of the configuration where the restrictions were placed 10 diameters upstream from the tube orifice.

IV. C. 2. Results

The data obtained for the drop patterns of the different restrictions are given in fig. IV. 6 and 7 and in table IV. 3, 4 and 5

when the restrictions were placed 10 and 40 diameters upstream from the orifice, respectively.

An overall comparison between the two pulse height distributions indicates a slight shift to the larger drops for the L/D = 10 curve compared with the L/D = 40 curve of the same restriction. When placed at a distance L/D = 10 from the orifice, the restrictions show differences in the pulse height distribution, which are greater than observed with restriction 5 in different locations.

Translating the differences in the curves to the effect of different size and shape of a restriction on the drop pattern is difficult. In general, it can be said that any restriction placed at a distance of 10 diameters upstream from the tube orifice has a specific influence on the breakup pattern. When restriction 2, which has a greater throat than the other restrictions is not considered, the influence of the upstream or downstream shape can be deducted as follows (fig. IV. 6):

If we assume, the downstream shape of a restriction is important, then restriction 1 and 3 should have almost the same effect on the drop pattern. The pulse height distributions show that this is not true. Thus the upstream shape can be important or a combination of upstream and downstream shape. If we assume, the upstream shape is important, then restriction 1 and 4 should have almost the same effect. The pulse height distribution indicates that this is nearly true. The curves of these restrictions are more similar than the curves of restriction 1 and 3. Thus the upstream shape of a restriction appears to be the dominant factor for the breakup pattern. The pulse height distribution for the restrictions when placed at a distance of 40 diameters from the tube orifice (fig. IV. 7) confirms the conclusion made above: the curves for the restrictions 3 and 5 are almost the same but are different from the curves for the open tube. The curves for restrictions 1 and 4, on the other, are nearly the same as for the open tube. Thus, the upstream shape leads to the most persistant effects.

In table IV. 3 the mean values andstandard deviations of some basic

variables are given. Again, there is no variable that can distinguish the different restrictions except restriction 2. In table IV. 4 and 5 the results of the discriminant analyses are given. Looking at the distribution of the misclassified groups, one notices that restriction 1 and 4 look like each other as do restriction 3 and 5.

The effect of the larger throat of restriction 2 seems to be a production of larger drops.

IV. D. The effect of self-exciting oscillations of the elastic restriction

Lissenburg found in his investigation of an elastic restriction; that under certain circumstances this restriction exhibited self-exciting oscillations. Similar sets of experiments has been done in this investigation.

IV. D. 1. Measurements

When the external pressure on the membrane of the elastic restriction had reached a value of about 6.10^3 N/m^2, a self-exciting oscillation of the membrane occurred. This could easily be observed by looking at the signal of the drop pattern on the oscilloscope. In addition a faint low frequency tone could be heard.
However, the whole system of oscillating elastic restriction and flow system wasn't stable. The amplitude of the oscillation decreased with time until the effect on the jet was no longer observable. After several attempts, one recording of three minutes duration of the drop pattern was made in which the phenomena were stable; the elastic restriction was 40 diameters upstream from the tube orifice. In addition to this stabilization problem, there occurred also a construction problem; no two elastic restrictions could be constructed to give the same properties.

IV. D. 2. Results

The pulse height distribution for the oscillating elastic restriction placed 40 diameters upstream from the tube orifice is given in fig. IV. 8. In the same figure also a distribution for the open tube is plotted. The distribution for the oscillating elastic restriction also shows a pattern with two modes. These modes are more slender than those of the open tube, thus the jet breaks up more into preferential drops. This is especially pronounced in the mode for the larger drops.

The oscillation of the flow field forces the jet to break up in smaller "bigger drops" (the shift to the left of the bigger drops mode). Thus an oscillation of the flow field leads to such a strong initial disturbance at the tube orifice that, even if this gives a wave length much smaller than the most unstable one (the Rayleigh wave length), this disturbance controls the jet breakup pattern.

IV. E. The effect of the fossa navicularis and elliptical meatus

Lissenburg has found that the effect of the fossa navicularis and elliptical meatus is to damp the turbulent energy across the entire wave number space.
It has been assumed, therefore, that the fossa navicularis and elliptical meatus on the jet breakup pattern should show a same effect. Differences in drop pattern caused by differences in restrictions or location of the restriction should stay the same therefore or should be less. Thus only the effect of the fossa navicularis and elliptical meatus on the drop pattern of the tube without restrictions has been studied. This has been done in combination with an examination of the influence of the jet velocity on the drop pattern.

IV. E. 1. Measurements

First, a five minutes recording of the drop pattern was taken

with the Reynolds number for the 5 mm diameter tube set at 4000. Then the fossa navicularis and elliptical meatus were coupled to the tube, the L.D.S. was lowered to compensate for the added length of the fossa navicularis and elliptical meatus. Again a five minute recording was taken of the drop pattern of this configuration; the Reynolds number was the same. This sequence was then repeated for Re_D = 5500 and Re_D = 8500.
The drop pattern from the fossa navicularis and the elliptical meatus showed a significant difference from those of the open tube. This difference could be observed on the oscilloscope. The number of pulses increased and the pulses showed a more uniform shape and size.
Also was it noticed, by visual and stroboscopic inspection, that the breakup length of the jet shortened remarkable.

IV. E. 2. Results

The pulse height distribution of the drop pattern for the open tube cases are given in fig. IV. 9. The three curves all show a bimodal pattern, but with increasing Reynolds number the smaller drops mode becomes less important. The top of this mode decreases and shifts to the left and while the base stays almost the same the mode becomes asymmetric. The mode of the bigger drops shows, with increasing Reynolds number, a flattening of the top while the maximum first decreases and then increases. The base of this mode first shifts and then widens. Thus, with increasing Reynolds number, the preferential size of the satellite drops decreases while the number of these small drops show a strong decrease. The preferential size of the big drops stays the same. However, the preference of the jet to break up into drops of the same size decreases (flattening of the mode).

The pulse height distribution for the fossa navicularis and elliptical meatus cases are given in fig. IV. 10. With increasing Reynolds number the bimodal pattern almost changes into an unimodal of only primarily drops. The two modes are almost symmetric. The top of

the smaller drops mode decreases and shifts to the right while the base stays the same. For the bigger drops the top of the mode also decreases but there is only once a shift of the top (Re_D = 4000 → 5500). The base increases with increasing Reynolds number. Upon comparing the two figures we can see that the effect of the fossa navicularis and elliptical meatus on the drop pattern consists of:

1) Producing a smaller size of the preferential drop for both the smaller and the bigger drops mode.

2) Decreasing the number of smaller drops and increasing that of the bigger drops.

3) Transferring the asymmetric modes of the open tube drop distributions to almost symmetric ones.

IV. F. Breakup length

A rough measurement of the breakup length of the jet was made for each of the experimental conditions described above. The distance from the tube orifice to the most probable breakup point was measured by a visual inspection of the jet with the stroboscope. For all the experiments with a flowrate of 15.7 ml/s the breakup length of the jet was 0.19 m $\pm$ 1%. This result (a constant breakup length) confirms the assumption that the gravity will not have a different effect on the different experiments. For example, if the breakup length for one experiment was much shorter or longer then there should be a gravitational influence on the breakup pattern due to the difference in jet diameter at the breakup point.

For the experiments with variable flowrate, the breakup length increased with increased Reynolds number. The following breakup lengths were measured (I.D. = 5 mm; L/D ≃ 60).

Re_D	breakup length
4000	0.21 m
5500	0.25 m
8500	0.38 m

These values have an almost linear relation, which indicates that for this experimental setup the jet lies in the turbulent region of fig. I. 1.

The effect of the fossa navicularis and elliptical meatus was a decrease in the breakup length, compared with the open tube. The relation between breakup length and Reynolds number again is linear.

Re_D	breakup length
4000	0.17 m
5500	0.21 m
8500	0.32 m

V. Succeeding investigations

When the effect of different restrictions on the jet breakup was studied (chapter IV. C), the analysis of the recorded data showed a significant difference for two of the five investigated restrictions, for both the locations L/D = 10 and 40 diameters distance from the tube orifice. Restrictions 2 and 4 showed an anomalous behaviour, especially in the pulse height distribution.
As Lissenburg did not investigate the effects of restriction 3 and 4 on the pipe turbulence, these measurements were taken as a part of this study. The apparatus and procedures were identical to those used by Lissenburg. The results are given in fig. V. 1 and 2 for the mean velocity and turbulent intensity profiles and the spectra of the turbulent energy for both the open tube and restriction 3 and 4.
In these experiments,no anomalous behaviour was found for restriction 4 compared with the open tube case. The conclusion of Lissenburg, that the more gradually a restriction diverges in downstream direction the more persistent the effects, has also been confirmed.
A further study of the anomalous behaviour of restrictions 2 and 4 (when water was used) revealed that the anomalous data occurred only in isolated segments of the recordings and that the isolated segments were sequential. That is, this behaviour was nor occurring intermittently but rather occurred only over one portion in each of the experiments with restriction 2 and 4. It was not possible to reproduce this behaviour in later experiments.

The anomalous data have been analyzed separately and the pulse height distributions data are given in fig. V. 3 together with the pulse height distribution for the self-exciting oscillation of the elastic restriction. From the similarity of the curves it is concluded that a spontaneous oscillating flow field is possible downstream from a restriction and that this oscillation can effect a change in the jet breakup. For the elastic restriction an external pressure of

6.10^3 N/m^2 was needed to effect a same behaviour of the jet. It is assumed, therefore, that such an anomalous behaviour of the jet is due to the existence of a more or less discrete eddy, persisting with distance downstream from the restriction. A physical reason for the existence of such an eddy can be the following. Assume a two dimensional system. When the divergency of a restriction in downstream direction is greater than the angle of the "emerging jet" leaving the throat of the restriction, it is possible that the "emerging jet" tends to lie on at one side of the restriction. This will be caused by the under pressure in the liquid layer between "emerging jet" and the wall of the restriction. However, this is not a stable flow because for the same reason the "emerging jet" tends to lie on at the other side of the restriction. Thus an oscillating flow field is possible. In the three dimensional case it is also possible that in addition to this oscillation a rotation of the flow field occurs, which can lead to a very persistent eddy.

VI. Conclusions

First, the specific conclusions for each set of experiments will be drawn. Then the combined results from stage 1 and 2 will be discussed and final conclusions will be drawn.

VI. A. Specific conclusions

VI. A. 1. The effect of restriction 5 when placed 10, 20, 30, 40 and 50 diameters upstream from the tube orifice

A restriction located at a distance to the orifice less than 25 diameters has an influence on the jet breakup. Beyond this distance the effect rapidly decreases. However, at the location L/D = 50 there again appears to be a small effect. Because the effect on the drop pattern does not decrease monotonically with increasing distance of the restriction from the tube orifice, the localization of the restriction in the tube will be restricted to a qualification: The restriction has been placed at a distance to the tube orifice less than or greater than 20 diameters. For this qualification, the pulse height distribution provides the most important variables.

VI. A. 2. The effect of the different rigid restrictions when placed 10 and 40 diameters upstream from the tube orifice

The differences in breakup pattern for the different restrictions depend strongly on the location of the restriction. When the restrictions are placed at a distance of 10 diameters upstream from the tube orifice each restriction had his own effect, more or less. The restrictions with a diverging shape in upstream direction influence the breakup pattern most. At a distance of 40 diameters upstream from the tube orifice, the patterns for the different restrictions become almost the same. But still the two restrictions with a smooth diverg-

ing shape in upstream direction have most difference with the open tube.

VI. A. 3. The effect of self-exciting oscillation of the elastic restriction

Evidently, a self-exciting oscillation influences the jet breakup pattern. The oscillation causes the jet to break up into small drops, while the distance of the oscillating restriction from the orifice seems of little importance.
From the anomalous behaviour of the restrictions 2 and 4, it is evident that the initial oscillation can be very faint and yet control the jet breakup.

VI. A. 4. The effect of the fossa navicularis and elliptical meatus

The fossa navicularis and elliptical meatus, when attached to the open tube, alters the pulse height distribution from a bimodal (large "main" drops and small "satellite" drops) to a nearly unimodal distribution. This trend is more pronounced as the Reynolds number is increased. The main drop size is decreased; this is primarily an effect of the elliptical meatus.

VI. A. 5. Analysis of the recorded data

For investigations carried out on the breakup pattern of a liquid jet at a constant flowrate, the drop size distribution carries the most information.
To interpret the differences in breakup pattern for the different restrictions or locations a statistical analysis is necessary. (The differences in percentage correct classification for especial the experiments with changing location, can be the result of the differences in the two statistical analysis methods, which differences can have great effect

when the cases to classify are more or less equal. A further study of this problem is necessary.)

VI. B. Comparison between the experiments with air and water

The results from the experiments carried out in air show that some restrictions can be observed, at the centreline, as far as 40 diameters downstream from that restriction.
The experiments carried out with water still show some effect on the drop pattern when the restriction was placed at a distance of 50 diameters from the tube orifice. These two distances of 40 and 50 diameters have been the longest distance from the tube orifice for which location measurements have been taken.
The results for the influence of the size and shape of a restriction, however, do not agree between stage 1 and 2. In air the effects are more persistent the less the restriction diverges in downstream direction. For the experiments with water the restrictions which diverge in the upstream direction have the most persistent effects. The downstream geometry appears to have little effect.

When there is an oscillating source in the air flow field, the turbulent energy is transferred to the higher frequency eddies with distance downstream. For the experiments with water the pulse height distribution tends to shift the top of the main drops mode towards the bigger drops, with distance downstream.
In the experiments with air the fossa navicularis with elliptical meatus damps out the turbulent energy across the entire wave number space but this effect is especially pronounced at the low frequency range.
For water, the effect on the jet breakup is a more uniform distribution for the bigger drops. These bigger drops, however, are smaller than those of the tube without fossa navicularis and elliptical meatus; this is primarily an effect of the elliptical meatus.

When the turbulent energy spectra are compared with the pulse height distribution, especially for the experiments carried out on the fossa navicularis and the oscillating restriction, the following conclusion can be drawn. When the energy in the lower frequency range decreases the small drops become less in number (fossa navicularis) and when the energy in the lower frequency range increases, the drops become smaller (oscillating restriction). Moreover when one certain eddy in the lower frequency range has sufficient energy, this eddy will control the drop pattern (anomalous jet breakup).
This assumption is supported when the pulse height distribution and the energy spectra are compared for the experiments where the distance to the orifice has been increased (fig. IV. 4 and fig. V. 2). The energy spectrum shows, in the low frequency range, a decrease in energy compared with the open tube when the restriction has been placed within a distance of 10 diameters from the tube orifice. A maximum in energy for the low frequency range was reached at 20 diameters.
In the pulse height distribution the location L/D = 10 shows for both the right flank of the smaller drops mode and the left and right flank of the bigger drops mode a small shift to the right, compared with the open tube. For the location L/D = 20 only the left flank of the bigger drops mode shows a remarkable shift to the left.

VI. C. Final conclusions

The jet breakup pattern is influenced by a restriction located upstream from the orifice. The influences of the size, shape, and location, however, lead to much smaller differences in the drop pattern than is observed in the external urinary streams of human males, and can not be regarded as the dominant influence.

There exists a correlation between the results of the measurements with air and water. An alteration in the turbulent energy of the eddies, especially in the lower frequency range, causes a specific reaction in the breakup pattern.

A diverging shape in upstream direction of the restriction causes more effect on the jet breakup than does a restriction with a sharp edge in upstream direction.

The effect on the jet breakup caused by a restriction with a diverging shape in upstream direction is more persistent with distance downstream than the effect caused by a restriction with a sharp edge in upstream direction.

Periodic oscillations change the breakup pattern totally as does the fossa navicularis and elliptical meatus. However, the change is not the same.

To observe differences in the jet breakup pattern at a constant flowrate, the pulse height distribution is most important. The time interval distribution is of only minor interest. An intensive statistical treatment of the data is necessary to detect the effects of size, shape, and location of a restriction.

APPENDIX 1

Basic principles of the optical-electro transducer

The pulse height, caused by an interruption of the light sheet by a drop is linear with the amount of light intercepted. When the drops are assumed spherical the following relations can be calculated:

pulse height h (time)
width of the interruption l (time)
calibration factor cf

$$h(t) = cf.l(t) \qquad (1)$$

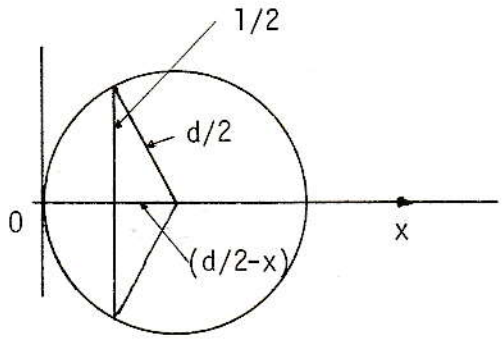

drop diameter d
direction of the drop x

$$\left(\frac{d}{2}\right)^2 = \left(\frac{l}{2}\right)^2 + \left(\frac{d}{2} - x\right)^2$$

or $$l = 2\,(d.x - x^2)^{\frac{1}{2}} \qquad (2)$$

drop velocity U
pulse width tw

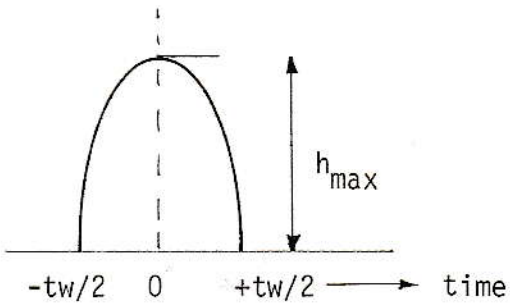

$$t = -\frac{tw}{2} \rightarrow x = 0$$

$$t = +\frac{tw}{2} \rightarrow x = d$$

and $$tw = \frac{d}{U} \tag{3}$$

$$x = (t + \frac{tw}{2})\ U \tag{4}$$

substitute in (2)

$$l\ (t) = d\left[1 - (\frac{2Ut}{d})^2\right]^{\frac{1}{2}} \tag{5}$$

substitute (5) in (1)

$$h\ (t) = cf.d\left[1 - (\frac{2Ut}{d})^2\right]^{\frac{1}{2}} \qquad |t| \leqq \frac{d}{2U} \tag{6}$$

$$= 0 \qquad \text{else}$$

Only for spherical drops the drop velocity can be calculated from the pulse

$$\text{for } t = o : h(o) = h_{max} = cf.d$$

Substitute (3) leads to:

$$U = \frac{h_{max}}{cf.tw} \tag{7}$$

If a jet breakup is assumed according to Rayleighs theory (linear), the drops will be separated by equal distances

$$\lambda^* = 4.51\ D_j$$

and $$d = 1.89\ D_j$$

Then the time interval between two drops will be

$$t_i - t_{i-1} = \frac{\lambda^*}{U} \tag{8}$$

and the ratio of the pulse interval (= time interval) and the pulse width

$$\frac{\lambda^*}{U} \Big/ \frac{d}{U} = \text{constant} \tag{9}$$

Appendix 2

Estimation of the initial disturbance amplitude

From the linear theory of the jet breakup (Rayleigh, 1878) we find for the jet length

$$L_B = \frac{\bar{U}_j}{\mu^*} \ln \frac{D_j}{2\delta_0}$$

where L_B is the breakup length, $\bar{U}_j$ the jet velocity, D_j the jet diameter, μ^* the growth rate for the most unstable disturbance and δ_0 the initial amplitude of the disturbance. Most experiments with laminar jets show that $\ln \frac{D_j}{2\delta_0}$ has a value of the order of 12.

The growth rate of the most unstable disturbance is found to be

$$\mu^* = \left(\frac{\sigma}{\rho D_j^3}\right)^{\frac{1}{2}}$$

with $\sigma = 73.10^{-3}$ N/m

$\rho = 1000$ kg/m^3

$D_j = 4.10^{-3}$ m

we find $\mu^* \simeq 34$ s^{-1}

In our experiments we have

$$\bar{U}_j = 1.25 \text{ m/s and } L_B \simeq 0.19 \text{ m}$$

so that

$$\ln \frac{D_j}{2\delta_0} = \frac{\mu^* L_B}{\bar{U}_j} \simeq 5$$

and $\delta_0 \simeq 1.10^{-5}$ m

For a comparable laminar jet we find $\delta_0 \simeq 1.10^{-8}$ m. Thus the initial amplitude of the disturbance for a turbulent jet is about 1000 times that for a laminar jet.

Acknowledgements

This investigation was carried out in the Urodynamics Laboratory, Department of Urology, Academic Hospital Leiden, The Netherlands, under direction of Dr. Arthur M. Sterling. I greatly appreciated Dr. Arthur M. Sterling for his helpful discussions during the project and for his assistence in the preparation of this manuscript.
Further, I greatly appreciated Prof. Dr. P.J. Donker for reserving willingly room and funds for this project.
The manuscript was typed by Ms. Jeanne van Nassau. Thanks for your patience.

REFERENCES

1. Campbell, M.F., and Harrison, J.H. 1970: "Urology".
2. Chen, T. 1964: Proc. Am. Soc. Civil Eng. (Hydraulic Div.) 90, HY 1.
3. Dityakin, Yu. F., 1954: Izvestiza Akademii Nauk. 10, 124.
4. Lafrance, P. 1975:"The capillary breakup of laminar liquid jets". Thesis, University of Virginia, Dept. of Physics.
5. Lissenburg, R.C.D. 1974:"The influence of rigid and elastic restrictions on turbulent pipe flow". Report, T.H. Delft (W).
6. Rayleigh, Lord. 1878: Proc. Lond. Math. Soc. 10, 4.
7. Sterling, A.M. 1975: J. Fluid Mech., 68, 477.
8. Weber, C. 1931: Z. Angew. Math. Mech. 11, 136.
9. Zande, E. van de, 1974:"Air entrainment by plunging water jets". Thesis, T.H. Delft (N).

SYMBOLS

c	excentricity $c = \sqrt{1-b^2/a^2}$, a and b the major and minor axis
cf	calibration factor
d	drop diameter
f	frequency; $f^* = \bar{U}_j/\lambda^*$
h	pulse height
l	width of the light field interruption
n	number of samples
t	time
tw	pulse width
D	tube diameter; D_d, drop diameter; D_j, jet diameter.
H	dimensionless pulse height
P	dimensionless pulse interval; $\hat{p} = jP$, $j = 1,2,3 \ldots n$
Q	flowrate
U	Eulerian velocity; $\bar{U}$, time mean value; u, turbulence component; $u' = \sqrt{\overline{u^2}}$, root mean square turbulence velocity component; subscripts j, t refer to jet and tube respectively.
V_d	drop volume
λ	wavelength; λ^*, most unstable wavelength
ν	kinematic viscosity
σ	surface tension
ρ	density; ρ_a, ambient density
τ	dimensionless time
Re	Reynolds number; $Re_D = \frac{\bar{U}_t D}{\nu}$
$\hat{We}$	Weber number based on the ambient density; $\hat{We} = \frac{\rho_a D_j \bar{U}_j^2}{\sigma}$
Sr	Strouhal number; $Sr = \frac{f D_j}{\bar{U}_j}$

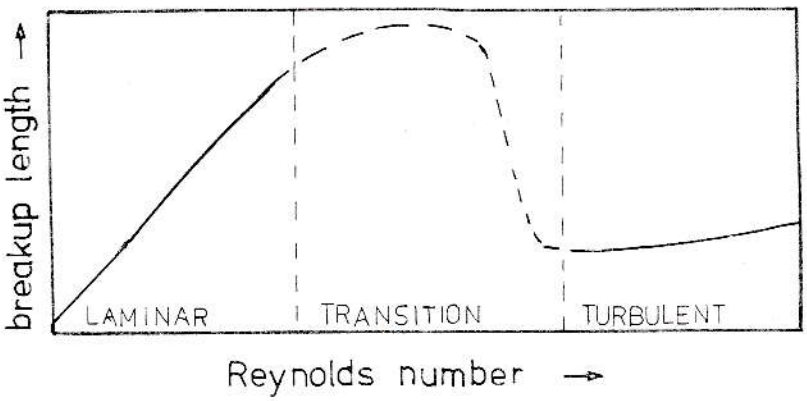

typical breakup curve

figure I. 1

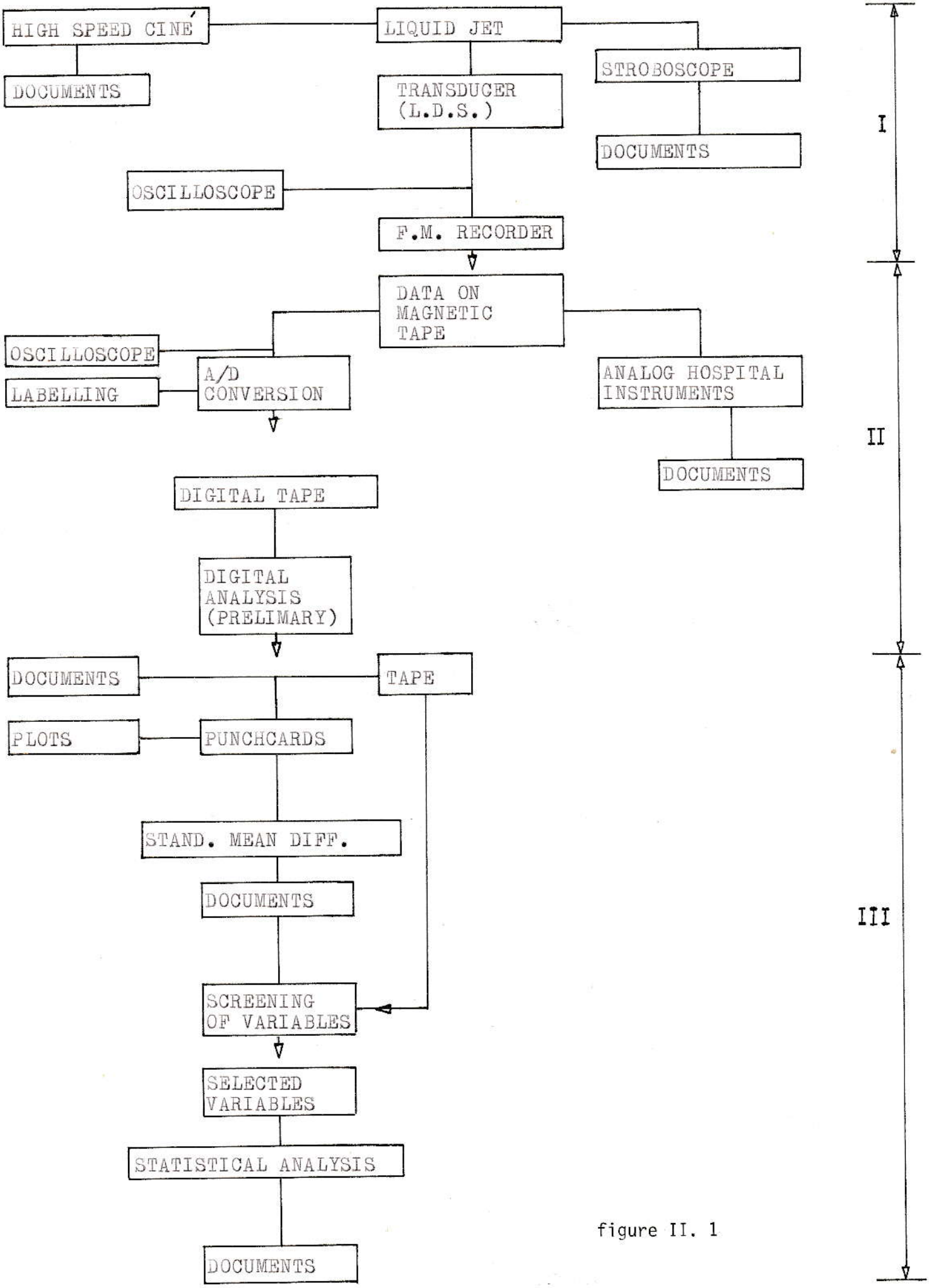
HIGH SPEED CINÉ
LIQUID JET
DOCUMENTS
TRANSDUCER (L.D.S.)
STROBOSCOPE
DOCUMENTS
OSCILLOSCOPE
F.M. RECORDER
DATA ON MAGNETIC TAPE
OSCILLOSCOPE
LABELLING
A/D CONVERSION
ANALOG HOSPITAL INSTRUMENTS
DOCUMENTS
DIGITAL TAPE
DIGITAL ANALYSIS (PRELIMARY)
DOCUMENTS
TAPE
PLOTS
PUNCHCARDS
STAND. MEAN DIFF.
DOCUMENTS
SCREENING OF VARIABLES
SELECTED VARIABLES
STATISTICAL ANALYSIS
DOCUMENTS
I
II
III

figure II. 1

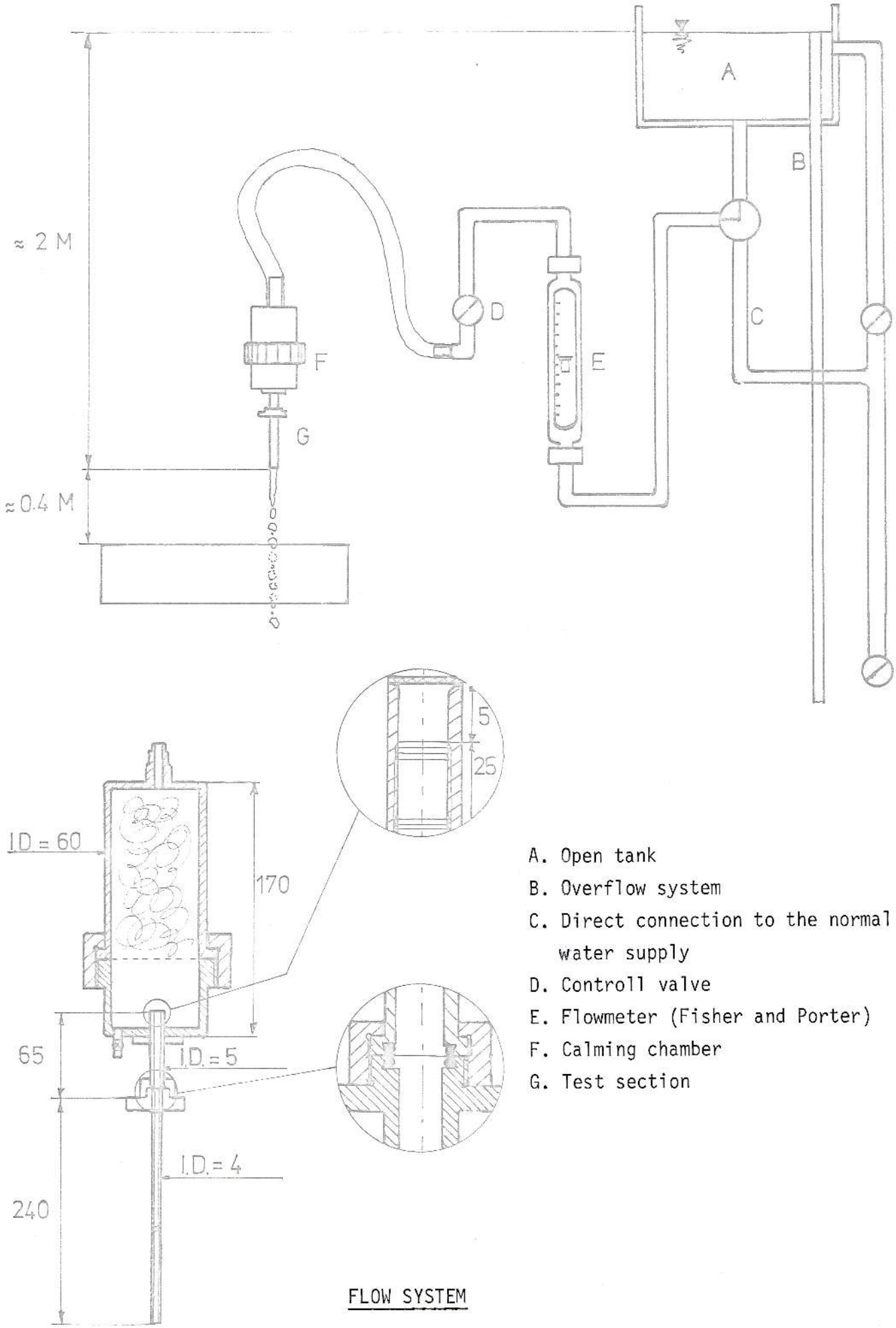

A. Open tank
B. Overflow system
C. Direct connection to the normal water supply
D. Controll valve
E. Flowmeter (Fisher and Porter)
F. Calming chamber
G. Test section

FLOW SYSTEM

figure II. 2

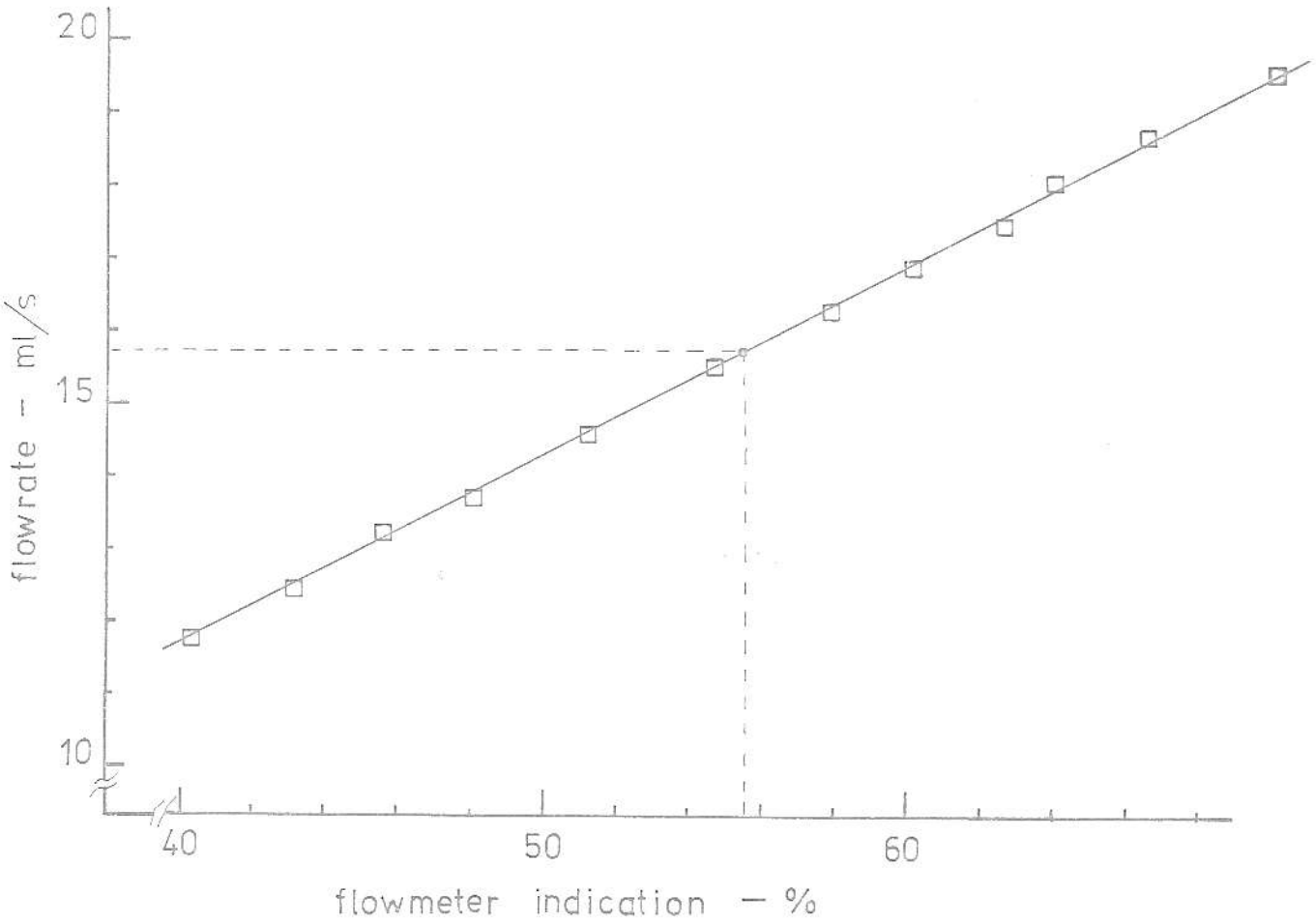

figure II. 3

RESTRICTIONS

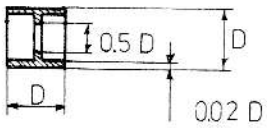

1

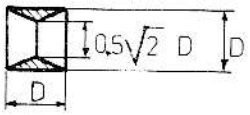

2

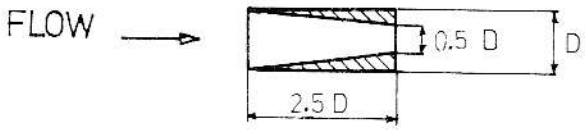

3

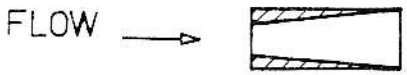

4

5

figure II. 4

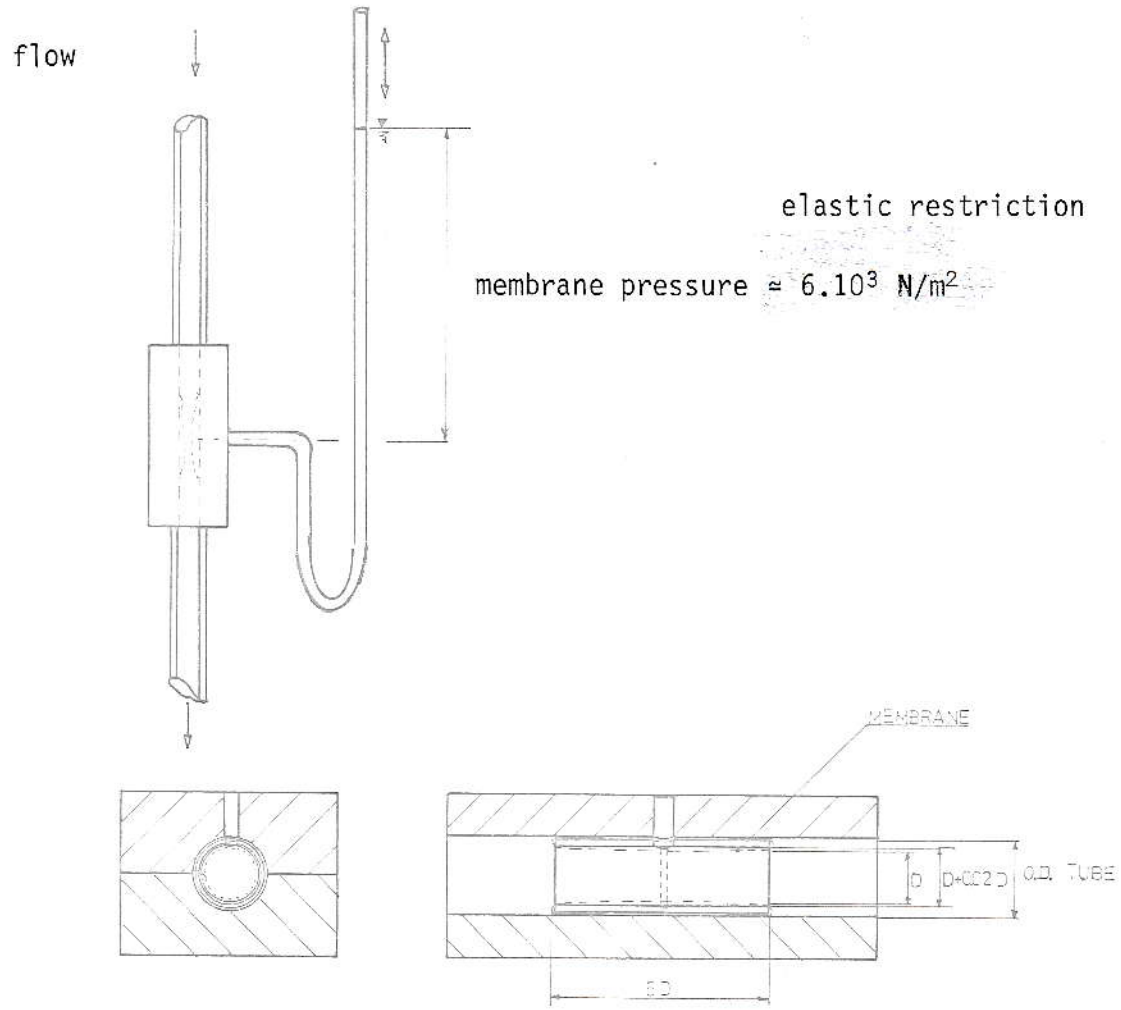

fossa navicularis with elliptical meatus

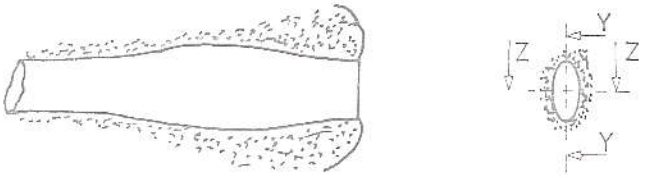

Profile Y-Y

$Y = -\cos\frac{\pi X}{2,5D} + 7$

$Y = -1,53\cos\frac{\pi X}{2,5D} + 6,53$

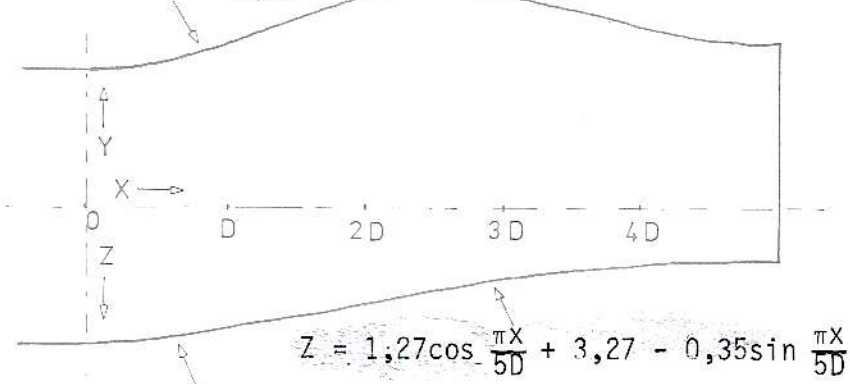

$Z = 1,27\cos\frac{\pi X}{5D} + 3,27 - 0,35\sin\frac{\pi X}{5D}$

$Z = 2,28\cos\frac{\pi X}{5D} + 2,72 - 0,07\sin\frac{\pi X}{5D}$

Profile Z-Z

figure II. 5

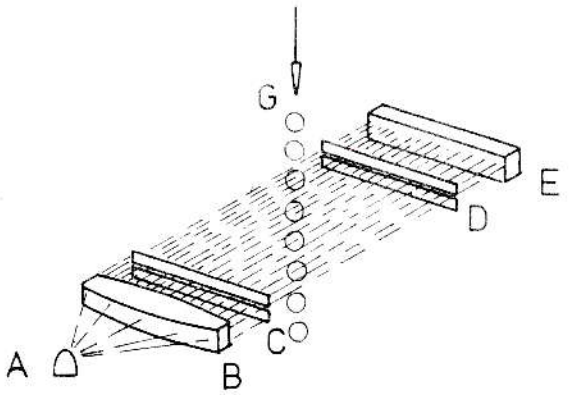

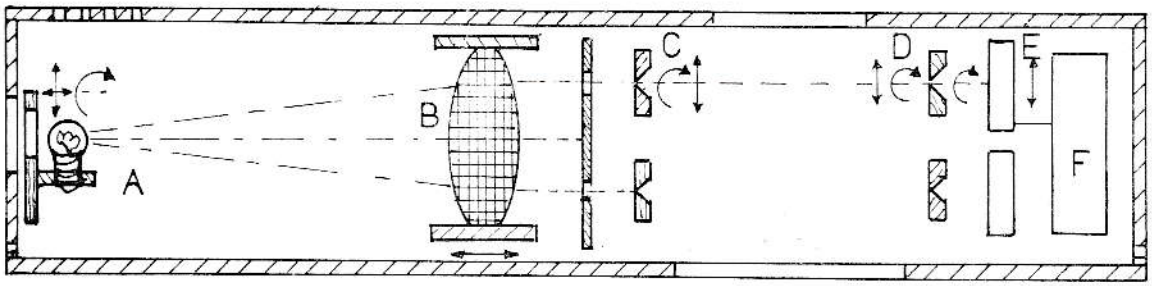

A. light source (Philips 7027 15V50W)
B. lens; doublet.
C, D. slits
E. photodiode (U.D.T. pin-L4)
F. amplifier (first stage)
G. drop train

LABORATORY DROP SPECTROMETER

figure II. 6

AMPLIFIER

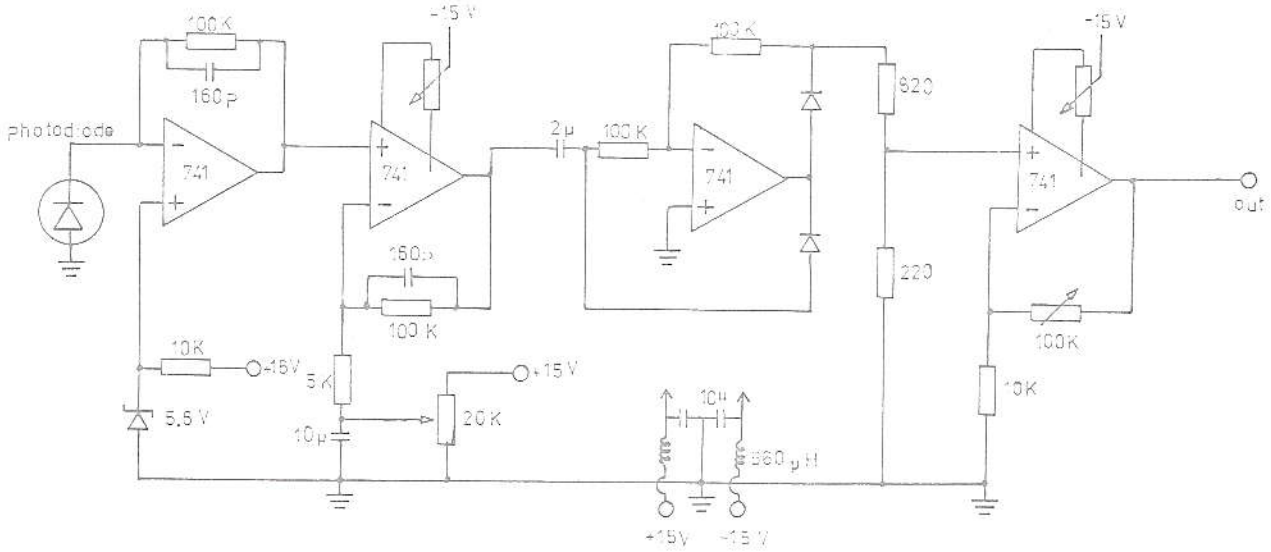

FREQUENCY RESPONSE

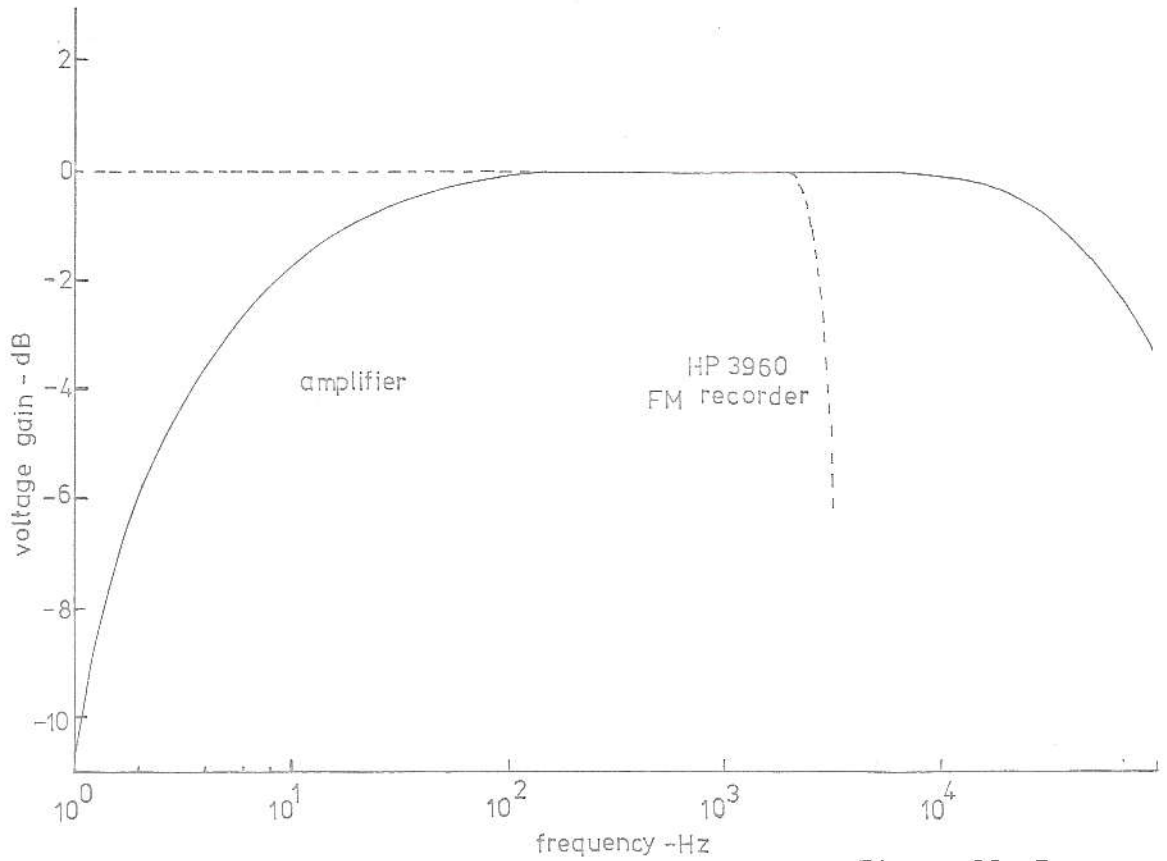

Figure II. 7

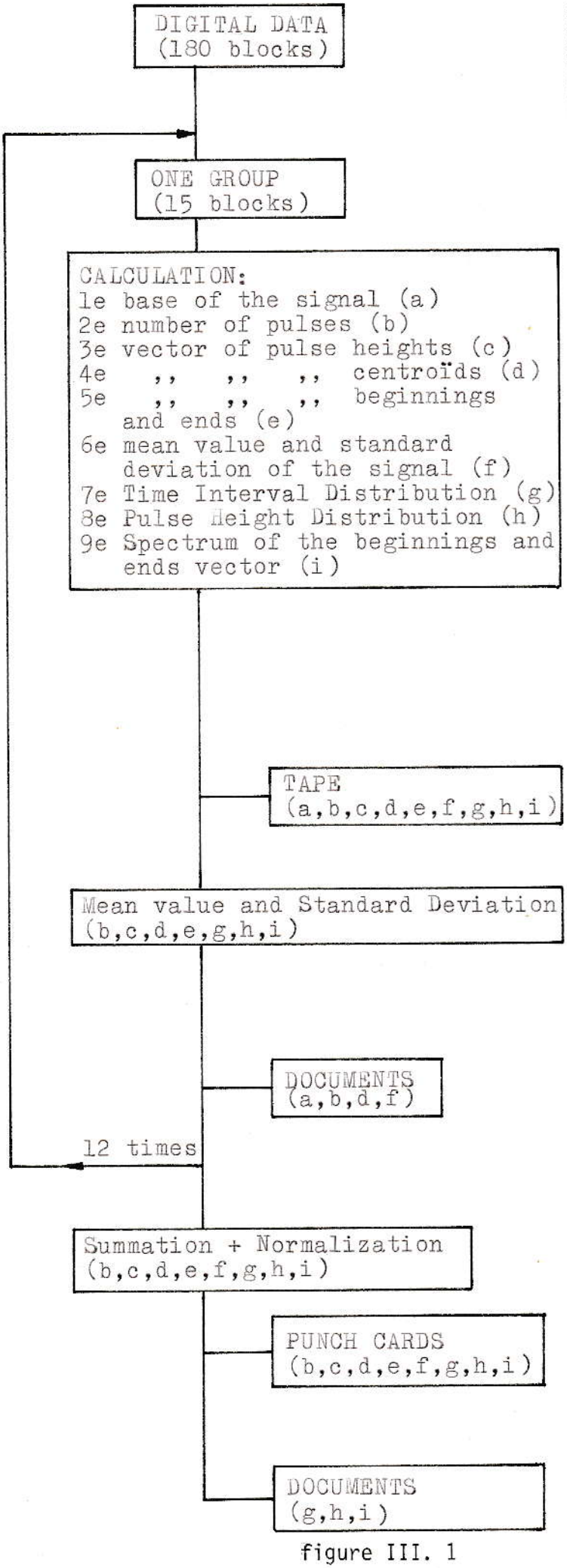

figure III. 1

L.D.S. signal (digital)

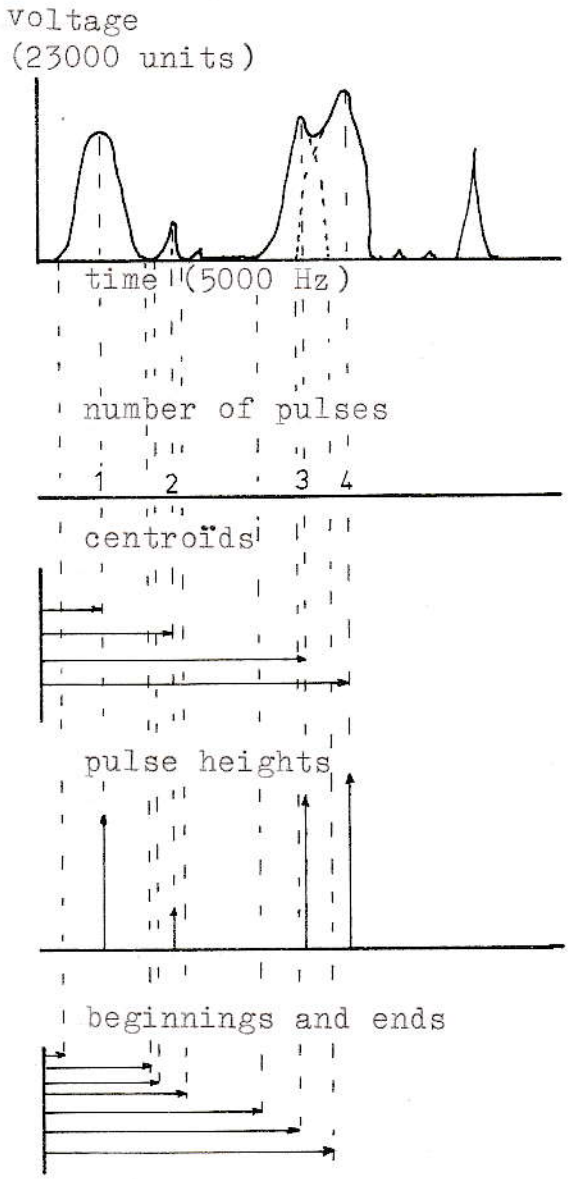

TYPICAL PLOTS

Time Interval Distribution

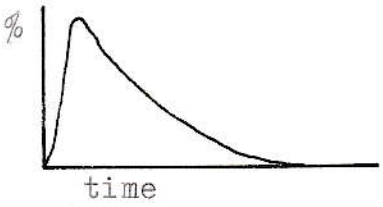

Pulse Height Distribution

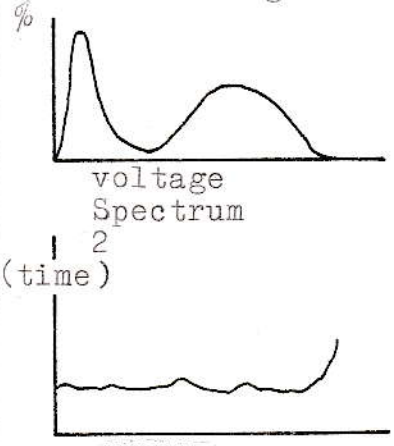

figure III. 2

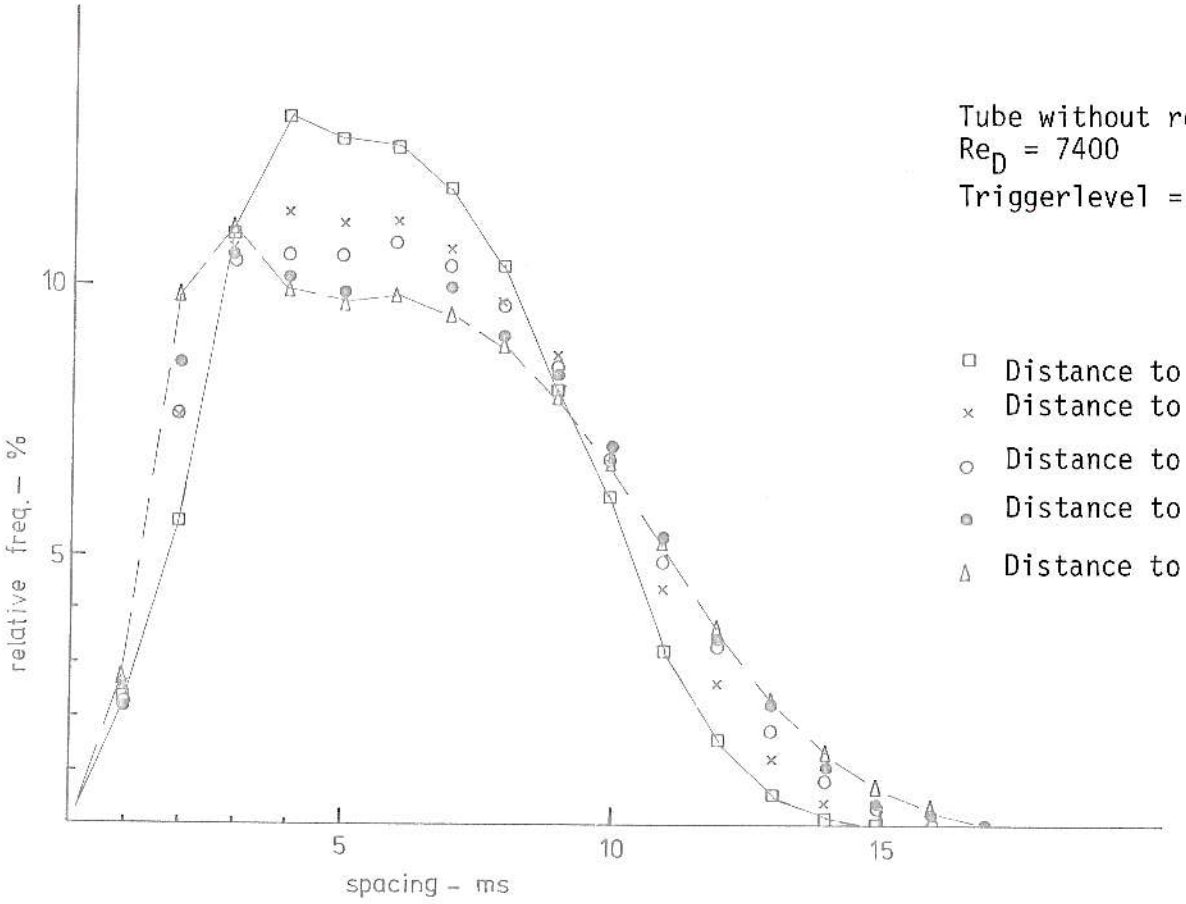

Tube without restriction.
Re_D = 7400
Triggerlevel = 0.25 V.

□ Distance to tube orifice 0.38 m.
× Distance to tube orifice 0.46 m.
○ Distance to tube orifice 0.54 m.
● Distance to tube orifice 0.62 m.
△ Distance to tube orifice 0.70 m.

figure IV. 1

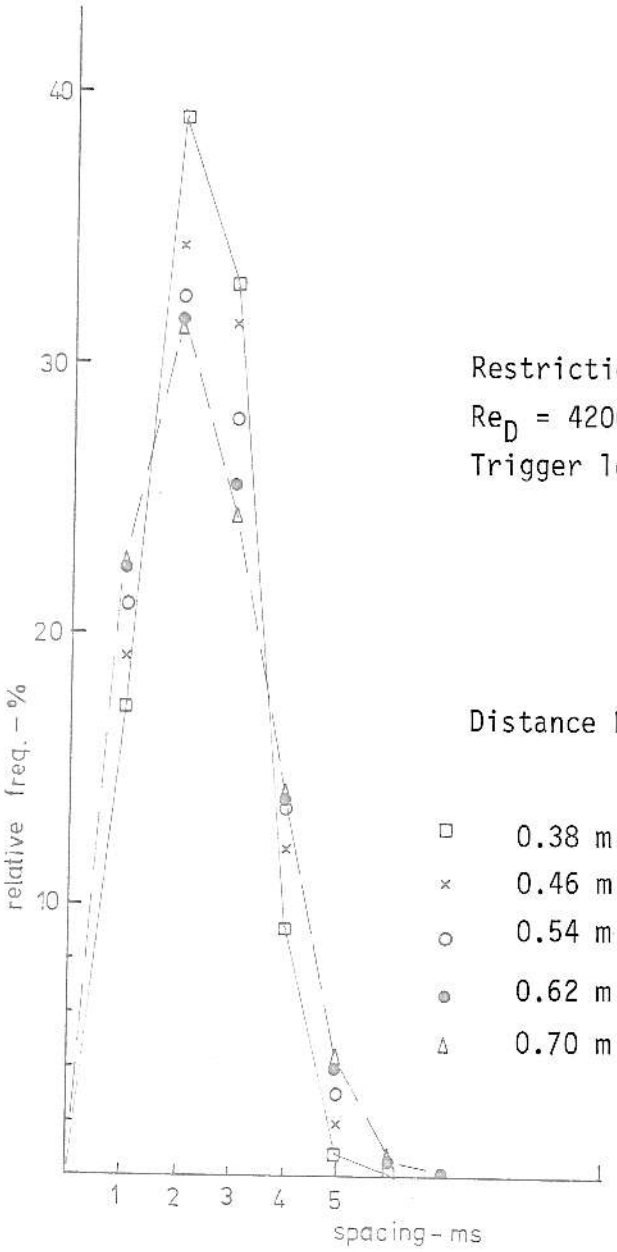

Restriction 1 placed at the orifice

Re_D = 4200

Trigger level = 0.25V

Distance L.D.S. to tube orifice

□ 0.38 m

× 0.46 m

○ 0.54 m

● 0.62 m

△ 0.70 m

figure IV. 2

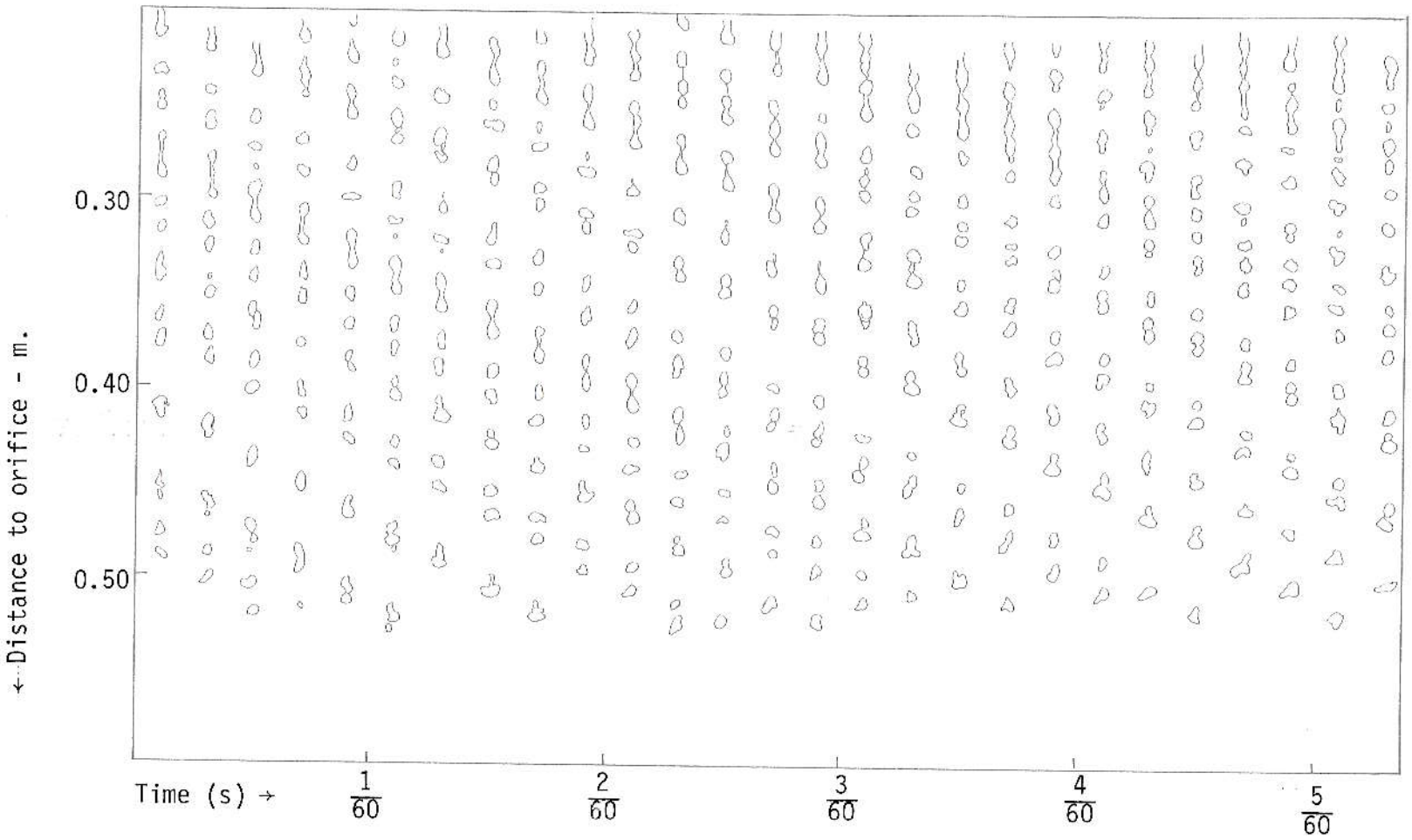

High speed ciné 3000 fr/s.
(only one in ten is drawn)
Tube without restriction; Re_D = 7400

figure IV. 3

Restriction 5 placed at several distances from the tube orifice; Re_D = 5000

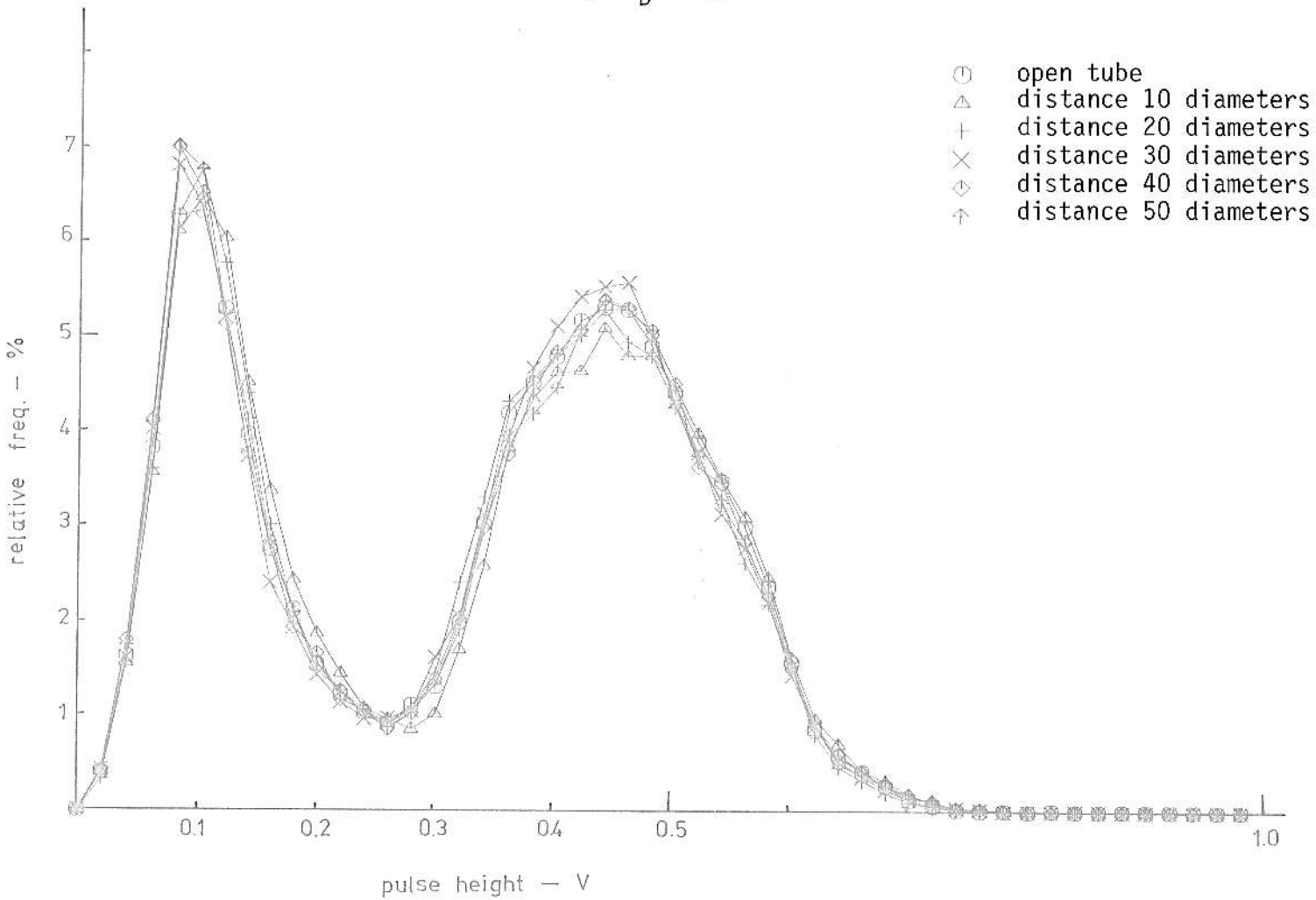

figure IV. 4

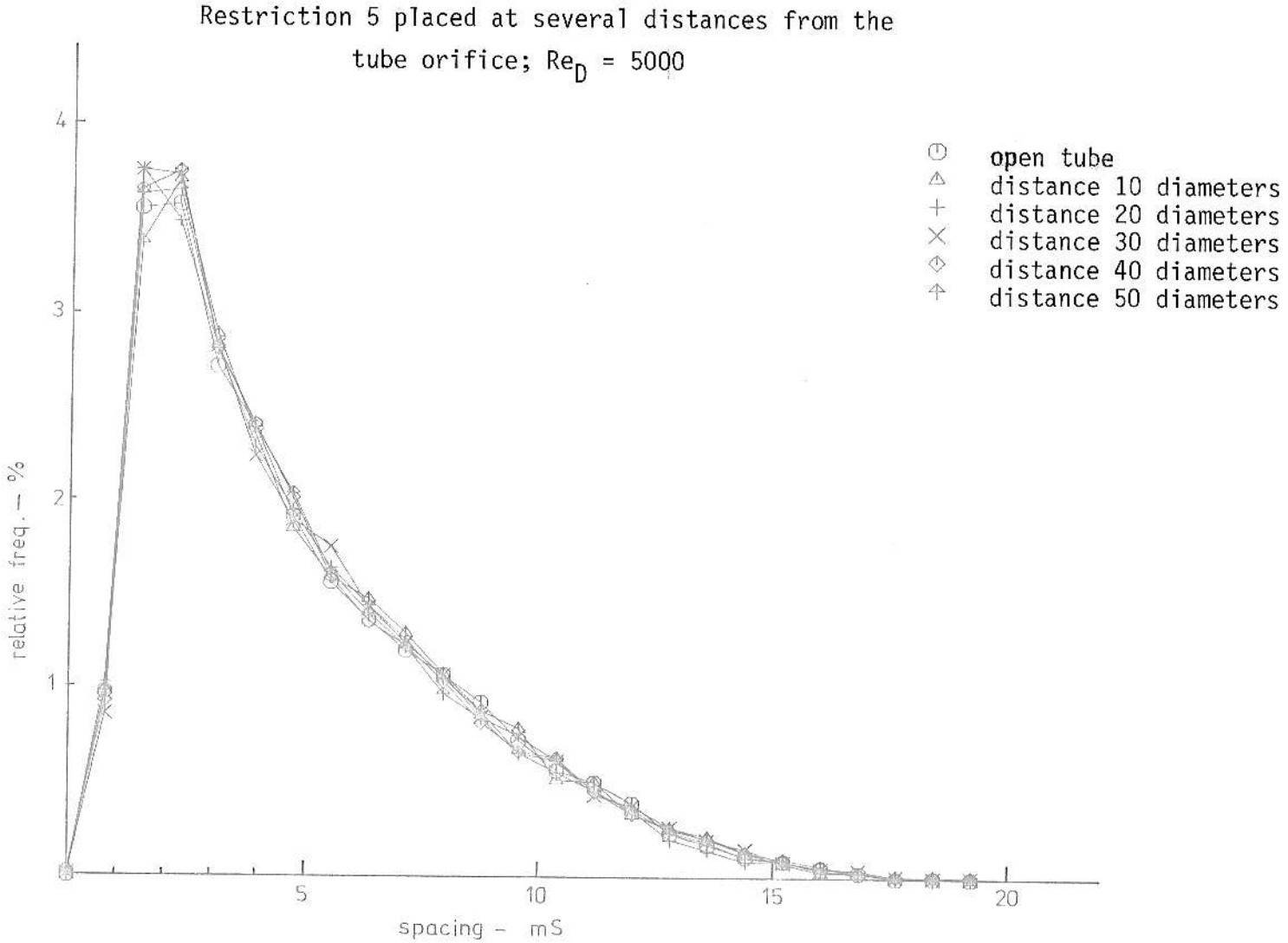
Restriction 5 placed at several distances from the tube orifice; Re_D = 5000
open tube
distance 10 diameters
distance 20 diameters
distance 30 diameters
distance 40 diameters
distance 50 diameters
relative freq. — %
spacing — mS
1
2
3
4
5
10
15
20

figure IV. 5

Mean value and standard deviation

(72 groups $\frac{1024}{5000}$ · 15 sec duration)

case	number of drops	time interval ($\times 10^{-4}$) sec	pulse height ($\times 10^{-2}$) volt	signal ($\times 10^{-2}$) volt	standard deviation of the signal ($\times 10^{-2}$) volt
0	605 ± 50	50 ± 4	33 ± 1	56 ± 4	52 ± 3
1	598 ± 41	51 ± 3	33 ± 1	57 ± 3	53 ± 2
2	618 ± 51	49 ± 4	33 ± 1	55 ± 4	52 ± 2
3	600 ± 44	51 ± 4	33.3 ± 0.6	57 ± 4	53 ± 3
4	607 ± 50	50 ± 5	33.4 ± 0.2	56 ± 4	57 ± 4
5	614 ± 33	50 ± 2	33.1 ± 0.8	55 ± 2	53 ± 4

Restriction 5 placed at a distance of 10, 20, 30, 40, and 50 diameters upstream from the orifice (open tube = case 0, L/D = 10 = case 1, etc.)

Table IV. 1

Linear discriminant analysis

35 variables, 48 groups

A (after 10 var.)

Allocated case \ True case	1	2	3	4	5
1	32	4	4	3	4
2	9	34	3	5	7
3	1	0	20	12	7
4	2	5	16	16	4
5	4	5	5	12	26

B (after 35 var.)

Allocated case \ True case	1	2	3	4	5
1	38	3	3	2	1
2	5	37	1	2	4
3	1	3	30	8	7
4	0	2	9	24	6
5	4	3	5	12	30

15 pulse height variables, 48 groups

C (after 15 var.)

Allocated case \ True case	1	2	3	4	5
1	30	9	5	4	6
2	6	30	7	0	6
3	4	5	22	14	6
4	3	0	9	19	10
5	5	4	5	11	20

Non-linear discriminant analysis

10 variables, 40 groups

D (after 5 variables)

Allocated case \ True case	1	2	3	4	5
1	19	2	1	2	4
2	7	26	6	5	2
3	2	6	17	6	3
4	1	3	3	10	2
5	11	3	13	17	29

Restriction 5 placed at a distance of 10, 20, 30, 40 or 50 diameters upstream from the orifice

(= case 1, etc. 5)

Table IV. 2

Re_D = 5000

Different rigid restrictions placed at a distance of 10 diameters upstream from the tube orifice

- open tube
- restriction 1
- restriction 2
- restriction 3
- restriction 4
- restriction 5

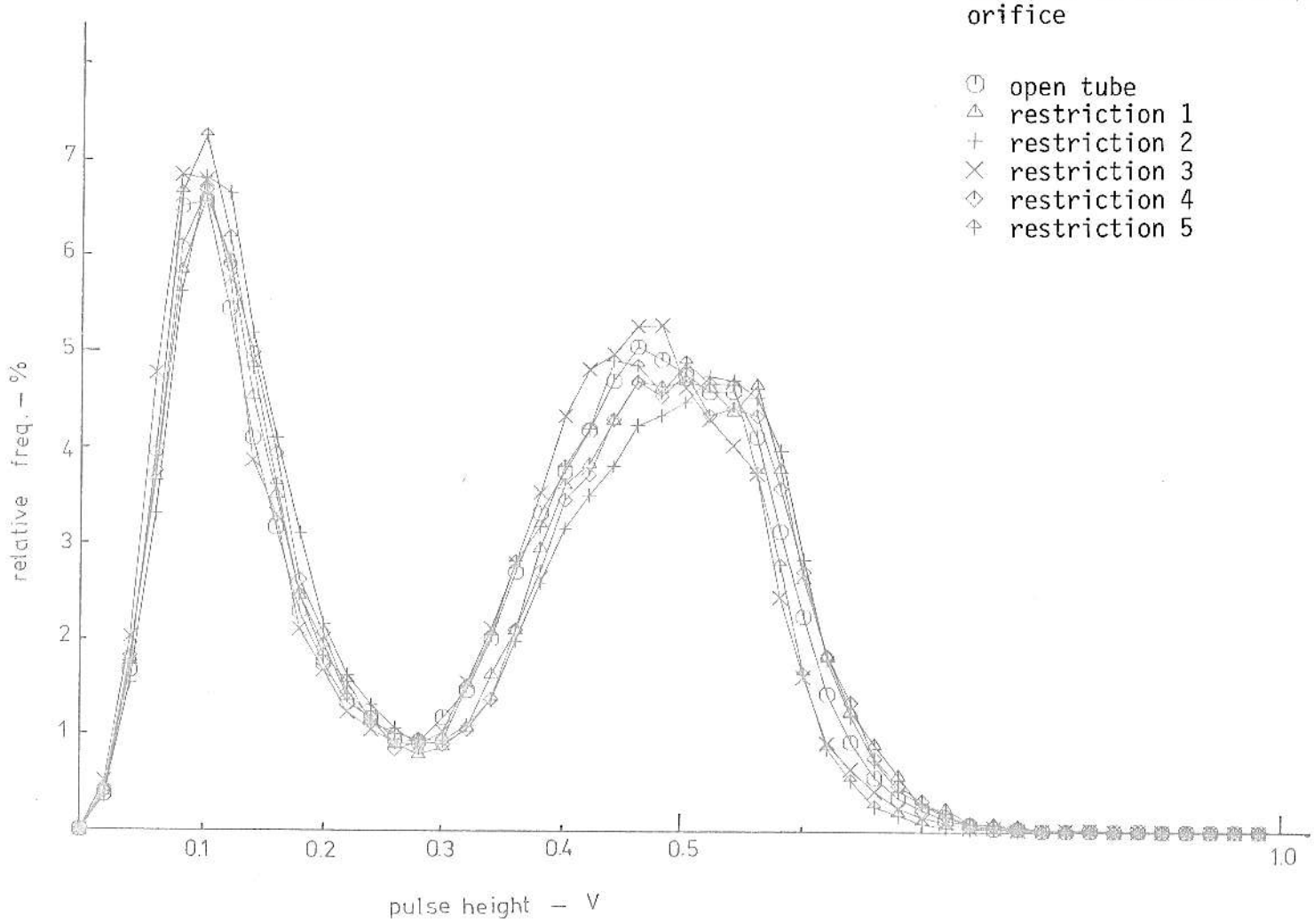

figure IV. 6

Re_D = 5000

Different rigid restrictions placed 40 diameters upstream from the tube orifice

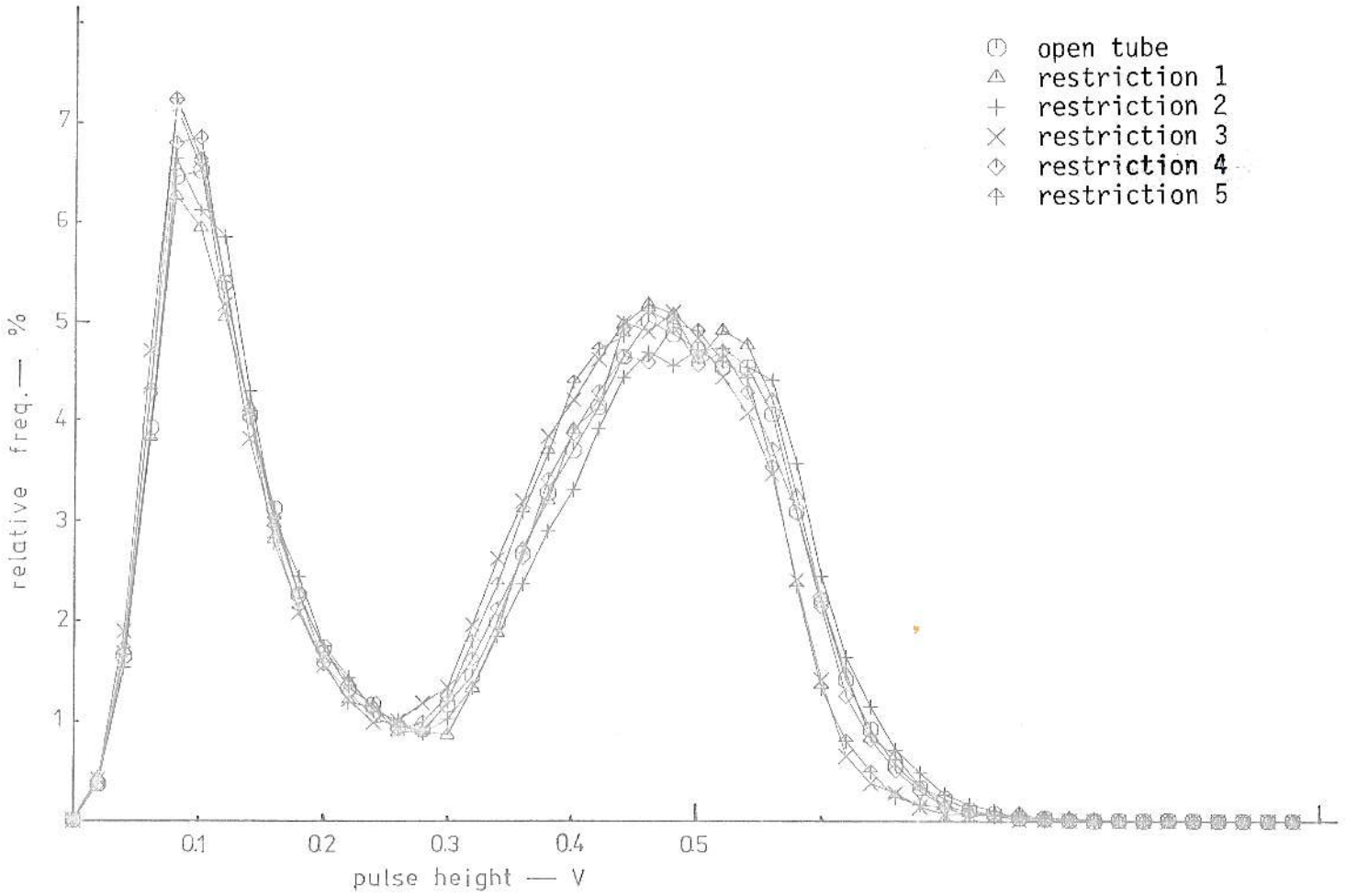

figure IV. 7

Mean value and standard deviation
(48 groups of $\frac{1024}{5000}$ 15 sec duration)

case	number of drops	time interval ($\times 10^{-4}$) sec	pulse height ($\times 10^{-2}$) volt	signal ($\times 10^{-2}$) volt	standard deviation of the signal ($\times 10^{-2}$) volt
L/D=10					
0	639 ± 17	49 ± 1	34 ± 1	53 ± 1	50 ± 3
1	617 ± 16	49 ± 1	35 ± 1	55 ± 1	51 ± 1
2	665 ± 13	46 ± 1	34 ± 1	51 ± 1	48 ± 2
3	612 ± 23	50 ± 2	33 ± 1	55 ± 2	52 ± 3
4	634 ± 21	48 ± 1	34 ± 1	53 ± 2	50 ± 3
5	649 ± 19	47 ± 1	33 ± 1	52 ± 1	48 ± 1
L/D=40					
0	639 ± 17	49 ± 1	34 ± 1	53 ± 1	50 ± 3
1	626 ± 19	49 ± 1	35 ± 1	54 ± 1	51 ± 2
2	647 ± 13	47 ± 1	35 ± 1	52 ± 1	50 ± 2
3	641 ± 12	47 ± 1	33 ± 1	53 ± 1	50 ± 2
4	640 ± 15	47 ± 1	34 ± 1	52 ± 1	49 ± 2
5	645 ± 17	47 ± 1	33 ± 1	52 ± 1	50 ± 3

Different restrictions placed at a distance of 10 and 40 diameters upstream from the tube orifice (open tube = case 0, restriction 1 = case 1, etc)

Table IV. 3

Linear discriminant analysis

35 variables, 48 groups

A (after 10 var.)

Allocated case \ True case	0	1	2	3	4	5
0	26	8	4	1	4	1
1	3	32	0	3	10	1
2	5	1	39	0	5	2
3	3	3	0	38	1	4
4	6	4	5	2	22	1
5	5	0	0	4	6	39

B (after 35 var.)

Allocated case \ True case	0	1	2	3	4	5
0	34	2	3	2	3	2
1	4	36	1	4	9	0
2	2	0	40	0	4	2
3	0	2	0	40	1	4
4	1	8	3	0	25	0
5	7	0	1	2	6	40

15 pulse height variables
48 groups

C (after 15 var.)

Allocated case \ True case	0	1	2	3	4	5
0	20	5	1	4	4	5
1	7	23	5	2	9	2
2	1	5	30	0	9	0
3	11	0	0	34	0	7
4	6	13	10	2	21	1
5	3	2	2	6	5	33

Non-linear discriminant analysis

10 variables, 40 groups

D (after 3 variables)

Allocated case \ True case	0	1	2	3	4	5
0	10	1	1	1	0	0
1	9	28	0	1	6	2
2	13	1	35	0	8	3
3	1	1	0	31	0	3
4	4	8	3	0	22	0
5	3	1	1	7	4	32

Different restrictions placed at a distance of 10 diameters upstream from the orifice

(open tube = case 0; restriction 1 = case 1 etc)

Table IV. 4

Linear discriminant analysis

35 variables, 48 groups

A (after 10 var.)

Allocated case \ True case	0	1	2	3	4	5
0	19	14	28	3	10	4
1	9	24	6	1	4	1
2	0	0	4	0	0	0
3	3	0	0	20	3	8
4	8	9	9	3	21	2
5	9	1	1	21	10	33

B (after 35 var.)

Allocated case \ True case	0	1	2	3	4	5
0	18	7	4	4	3	4
1	3	24	1	1	0	0
2	15	15	40	2	14	3
3	8	0	0	30	11	13
4	1	1	3	1	17	3
5	3	1	0	10	3	25

15 pulse height variables
48 groups
C (after 15 var.)

Allocated case \ True case	0	1	2	3	4	5
0	10	4	5	1	1	3
1	11	29	5	4	4	1
2	12	5	29	2	11	2
3	4	0	2	26	6	11
4	2	8	6	7	16	4
5	9	2	1	8	10	27

Non-linear discriminant analysis

10 variables, 40 groups

D (after 3 variables)

Allocated case \ True case	0	1	2	3	4	5
0	6	0	1	0	1	0
1	9	24	3	1	4	1
2	17	13	34	0	15	1
3	3	0	0	31	9	11
4	0	1	0	1	0	1
5	5	2	2	7	11	26

Different restrictions placed at a distance of 40 diameters upstream from the orifice

(open tube = case 0; restriction 1 = case 1, etc.)

Table IV. 5

Re_D = 5000

membrane pressure ≃ 6.10^3 N/m^2

Elastic vibrating restriction placed 40 diameters upstream

○ open tube
△ elastic restriction

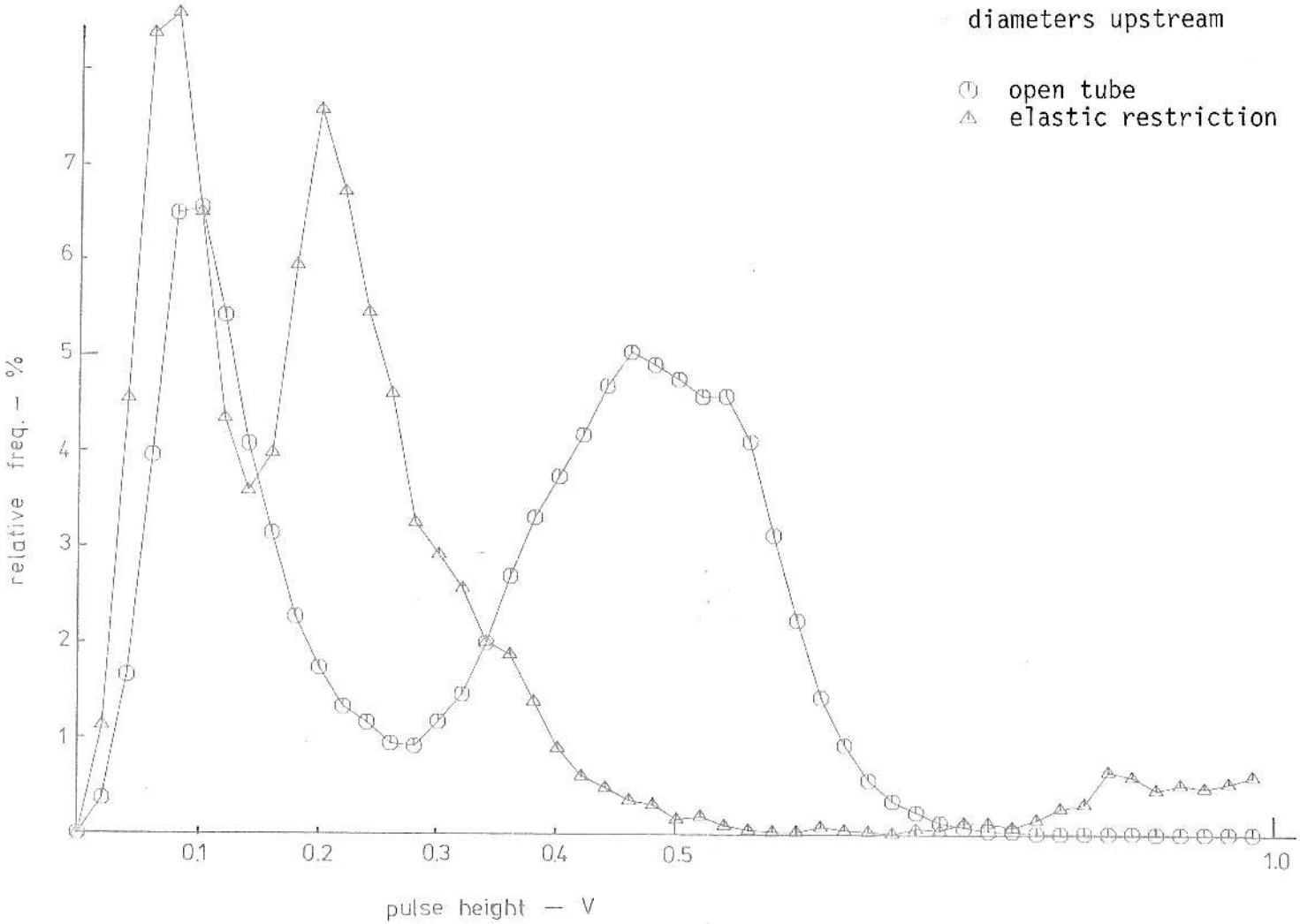

figure IV. 8

I.D. of the tube = 5 mm.
Tube without restriction

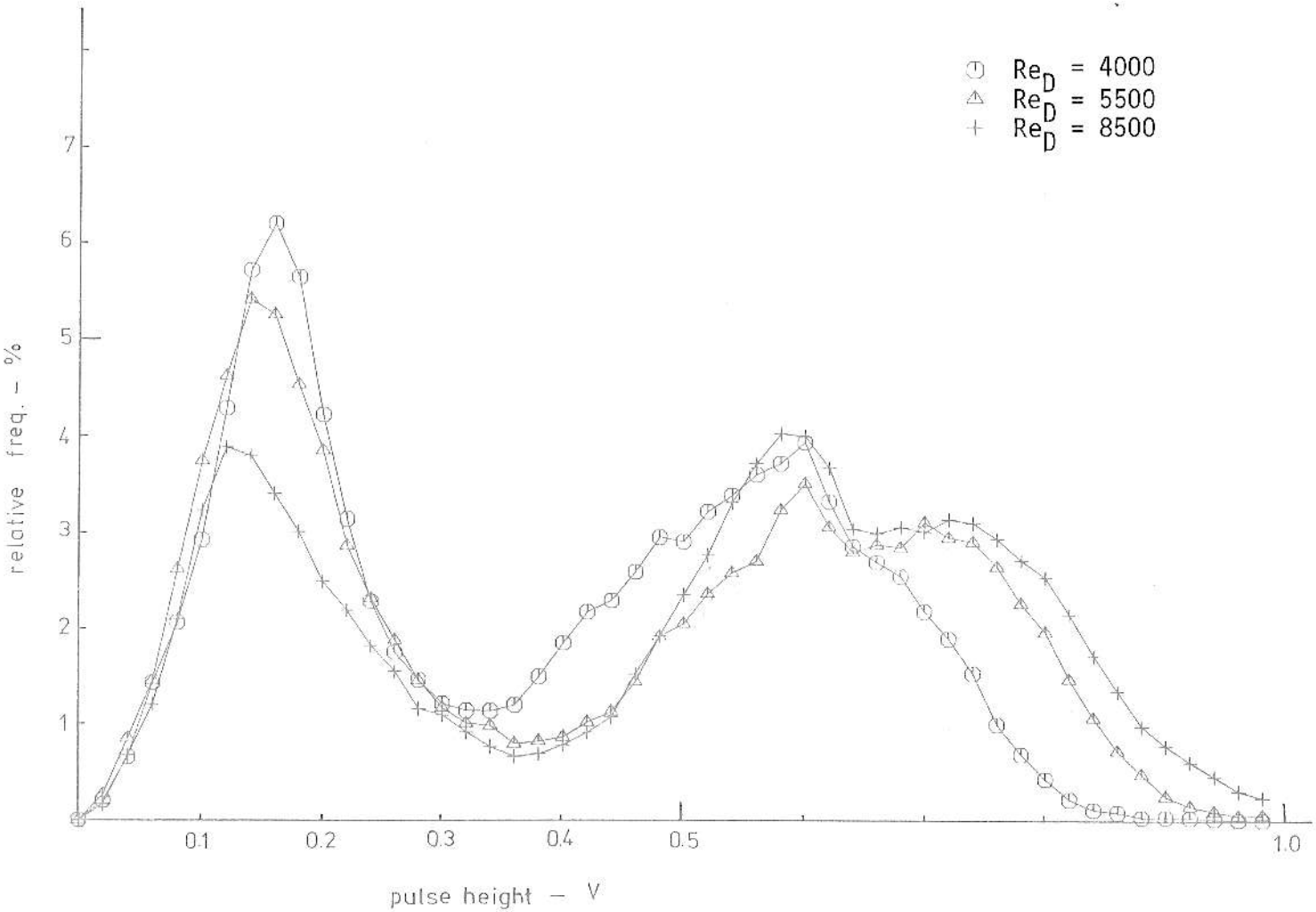

figure IV. 9

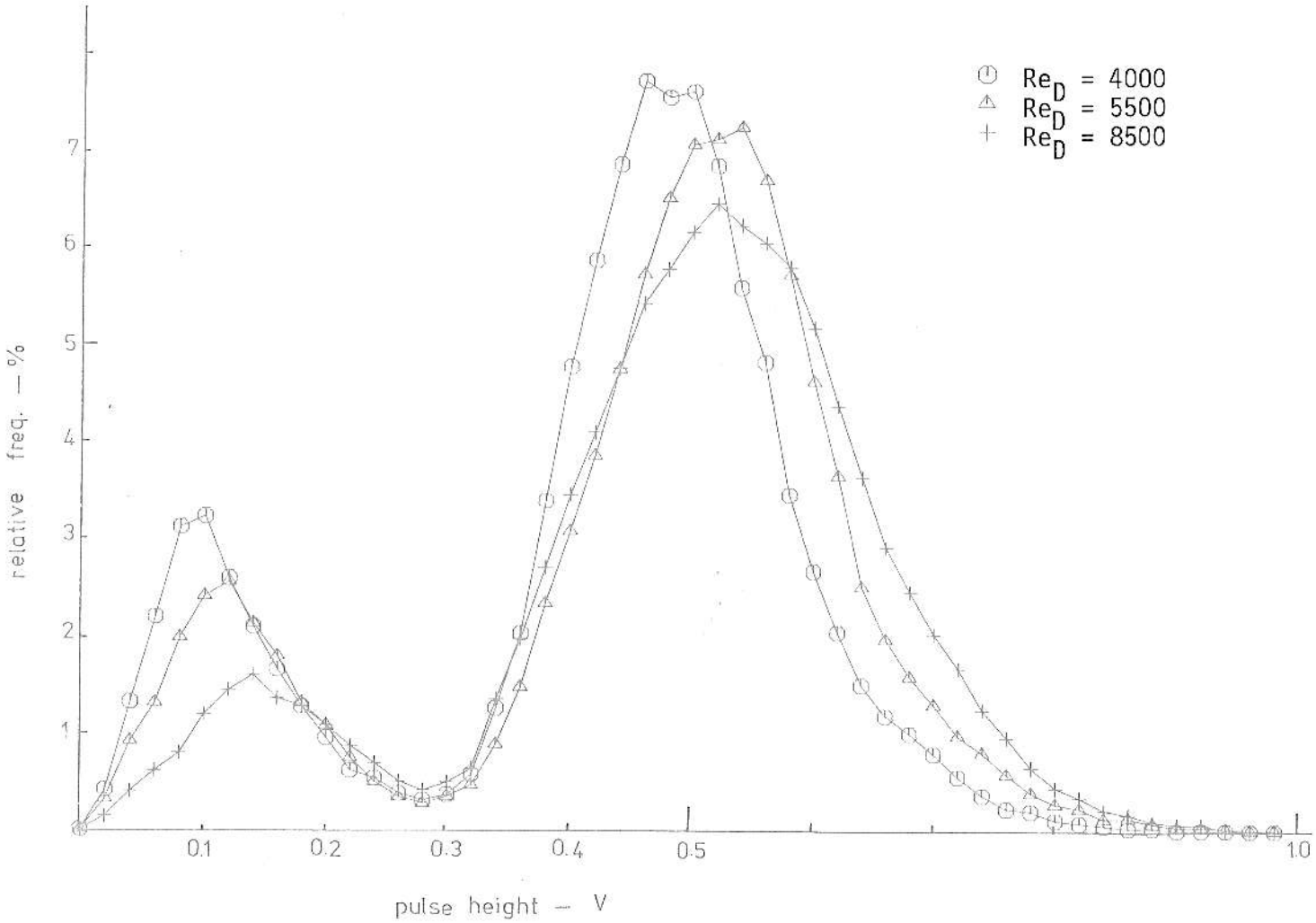
Tube I.D = 5 mm.
Fossa navicularis and elliptical meatus
Re_D = 4000
Re_D = 5500
Re_D = 8500
relative freq. — %
pulse height — V
1
2
3
4
5
6
7
0.1
0.2
0.3
0.4
0.5
1.0

figure IV. 10

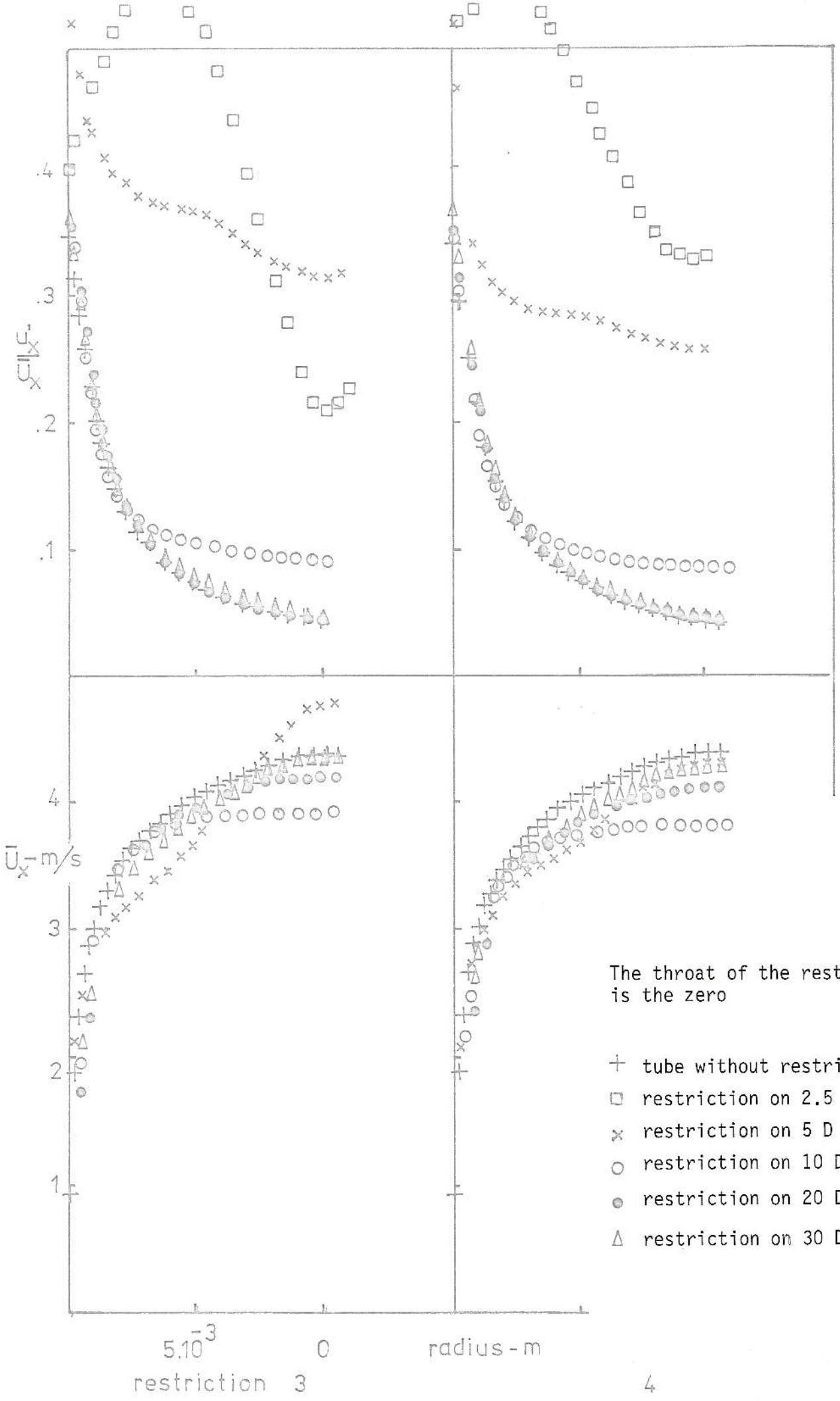
.4
.3
.2
.1
$\overline{u'_x}$
4
3
2
1
$\overline{U}_x$ - m/s
5.10^{-3}
0
radius - m
restriction 3
4
The throat of the restrictions is the zero
tube without restriction
restriction on 2.5 D
restriction on 5 D
restriction on 10 D
restriction on 20 D
restriction on 30 D

figure V. 1

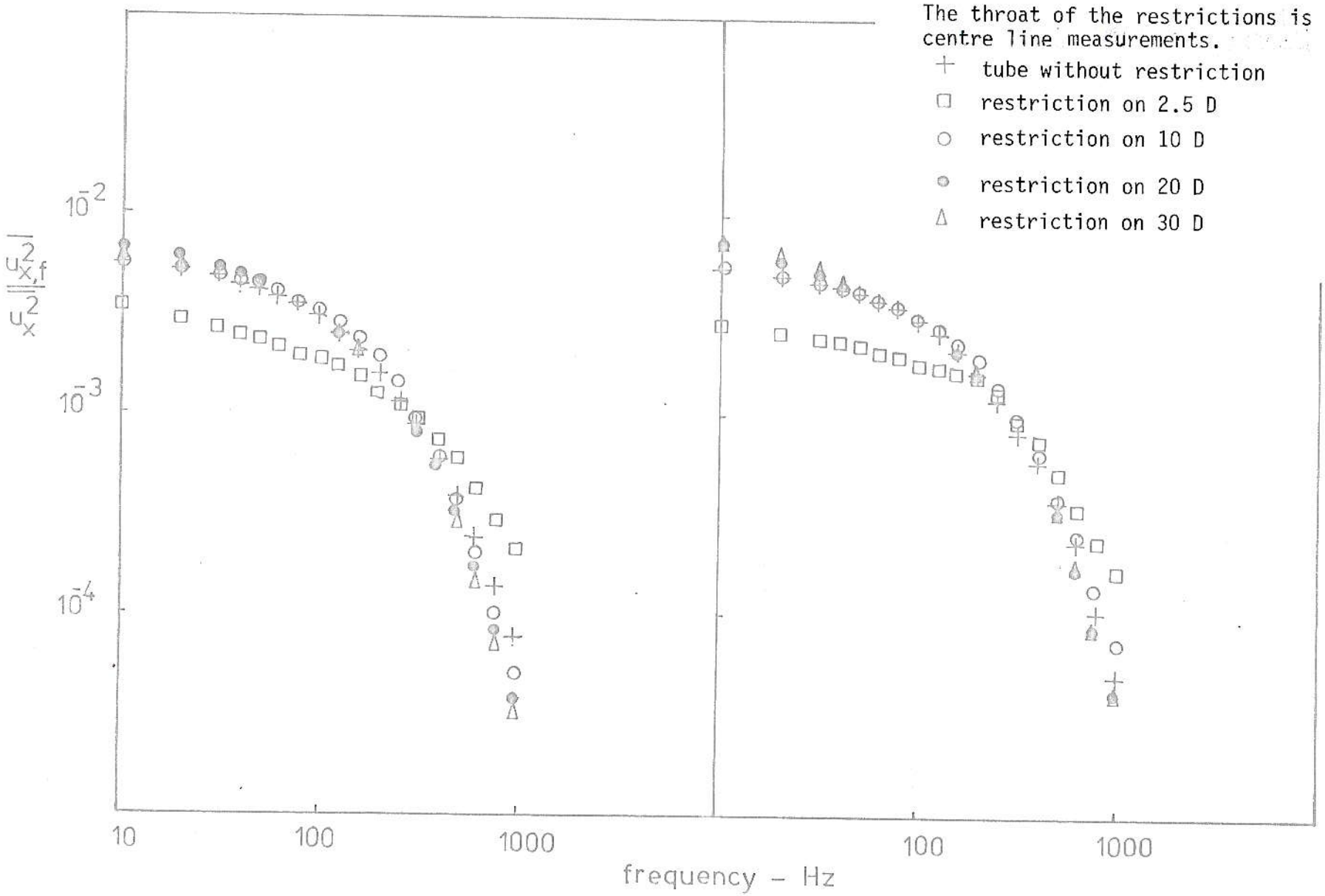
The throat of the restrictions is the zero.
centre line measurements.
tube without restriction
restriction on 2.5 D
restriction on 10 D
restriction on 20 D
restriction on 30 D
$\frac{\overline{u_{x,f}^2}}{\overline{u_x^2}}$
10^{-2}
10^{-3}
10^{-4}
10
100
1000
100
1000
frequency - Hz
restriction 3
4

figure V. 2

Re_D = 5000

Anomalous behaviour of restriction 2 and 4

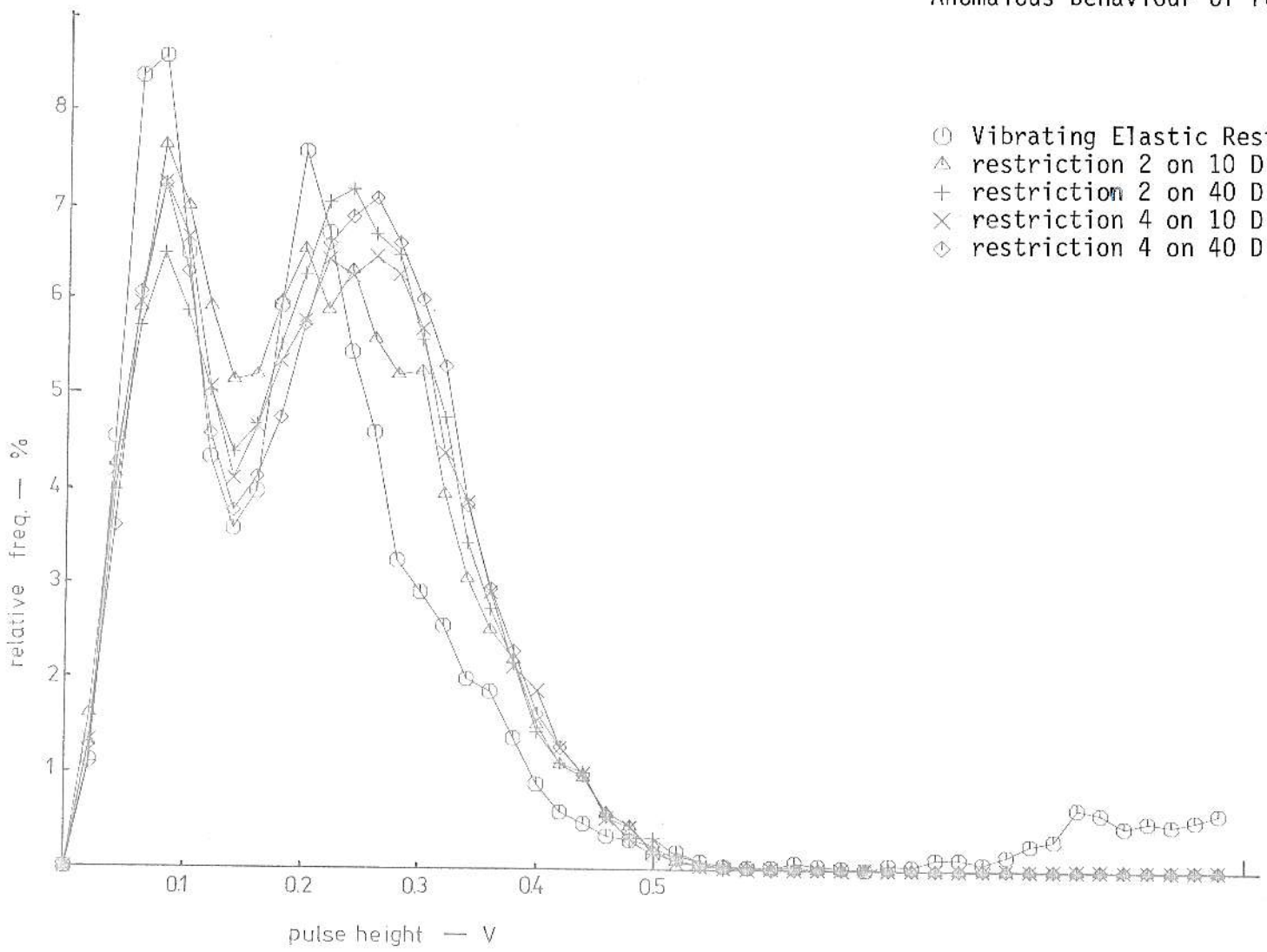

figure V. 3